

# Glaciological setting and structural evolution of the Shackleton Ice Shelf System, East Antarctica, over the past 60 years

Sarah S. Thompson,<sup>1,2\*</sup> Bernd Kulesa,<sup>2,3</sup> Adrian Luckman,<sup>2</sup> Jacqueline A. Halpin<sup>4</sup>, Jamin S. Greenbaum<sup>5</sup>, Tyler Pelle<sup>5</sup>, Feras Habbal<sup>6</sup>, Jingxue Gue<sup>7</sup>, Lenneke M. Jong<sup>8</sup>, Jason L. Roberts<sup>8</sup>, Bo Sun<sup>9</sup>, Donald D. Blankenship<sup>9</sup>

<sup>1</sup>Australian Antarctic Program Partnership, Institute for Marine and Antarctic Studies, University of Tasmania, Hobart, Tasmania, 7001, Australia

<sup>2</sup>Department of Geography, Faculty of Science and Engineering, Swansea University, UK

<sup>3</sup>School of Technology, Environments and Design, University of Tasmania, Hobart, TAS, 7001, Australia

<sup>4</sup>Institute for Marine and Antarctic Studies, University of Tasmania, Hobart, Tasmania, 7001, Australia

<sup>5</sup>Scripps Institution of Oceanography, University of California, San Diego, USA

<sup>6</sup>Oden Institute for Computational Engineering and Sciences, University of Texas at Austin, Austin, Texas, USA

<sup>7</sup>Polar Research Institute of China, Shanghai, China

<sup>8</sup>Australian Antarctic Division, Kingston, TAS, Australia

<sup>9</sup>Institute for Geophysics, University of Texas at Austin, Austin, TX, USA

Correspondence to: Sarah S Thompson (ss.thompson@utas.edu.au)

**Abstract.** The discovery of Antarctica's deepest subglacial trough beneath the Denman Glacier, combined with high rates of basal melt at the grounding line, have caused significant concern over its vulnerability to retreat. Recent attention has therefore been focusing on understanding the controls driving Denman Glacier's dynamic evolution, although knowledge of the wider regional context and timescales over which the future responses may occur remains incomplete. Here we consider the Shackleton system, comprising of the Shackleton Ice Shelf, Denman Glacier and adjacent Scott, Northcliffe, Roscoe and Apfel glaciers, about which almost nothing is known. We widen the context of previously observed dynamic changes in the Denman Glacier to the wider region of the Shackleton Ice Shelf system; with a multi-decadal timeframe and an improved biannual temporal frequency of observations in the last eight years (2014-22). We integrate new satellite observations of ice structure and airborne radar data with changes in ice front position and ice-flow velocities to investigate changes in the system. Over the 60-year period of observation, we find no evidence of either longer-term sustained change or significant annual or sub-annual variations in ice flow. A previously mapped increase in the ice flow speed of the Denman Glacier is not observable beyond 2008, and we do not identify any related change in the surface structure of the system since then. We do, however, observe more recent changes in Scott Glacier, with an acceleration in ice flow associated with calving that progresses from the ice front along the floating tongue since early 2020, but diminishes before the grounding line is reached. Consistently, no significant temporal variability in surface structure or ice flow speed are observed closer to the grounded ice. Given the potential vulnerability of the system to accelerating retreat into the overdeepened bedrock trough, better data recording the glaciological, oceanographic, and geological conditions in the Shackleton system are required to improve the certainty of

**Deleted:** Queen Mary and Knox coasts...hackleton Ice Shelf System, East Antarctica, over the past 60 years,... and implied dynamic stability of the Shackleton system ... [1]

**Deleted:** Stephen Cornford,<sup>2</sup>

**Formatted:**

**Formatted:** Superscript

**Formatted:** Superscript

**Formatted:**

**Formatted:** Superscript

**Deleted:** <sup>1</sup>

**Formatted:** Superscript

**Formatted:** Superscript

**Formatted:** Superscript

**Deleted:** the ...ntarctica's deepest subglacial trough beneath the Denman Glacier, combined with high rates of basal melt at the grounding line, have caused significant concern over its vulnerability to retreat. Recent attention has therefore been focusing on understanding the governing dynamic ...ontrols driving Denman Glacier's dynamic evolution, although knowledge of the wider regional context and timescales over which the future responses may occur remains poor...ncomplete. Here we consider the whole Shackleton system, comprising of the Shackleton Ii...e Ss ... [4]

**Deleted:** in...o the wider region of the Queen Mary and Knox coasts...hackleton Ice Shelf system; with a multi-decadal timeframe and an improved biannual temporal frequency of observations in the last eightseven...years (2014-21) ... [5]

**Deleted:** ,

**Deleted:** We furthermore use the BISICLES ice sheet model to assess the sensitivity and simulate the response times of the Queen Mary and Knox coasts to hypothetical disintegration of its floating ice areas, in response to coupled ocean and atmospheric forcing. Over the 60-year period of observation, the Queen Mary and Knox coasts do not appear to have changed significantly...we find no evidence of either longer-term sustained change or and higher frequency observations have not revealed any ...ignificant annual or sub-annual variations in ice flow. A previously observed ...apped increase in the ice flow speed of the Denman Glacier has not continued...s not observable beyond 2008, and we do can...ot identify any related change in the surface structure ...of the system since then. We do, however, observe more recent significant changes in the ...n Scott Glacier, with an acceleration in ice flow associated with calving and p...hat progressing...from the ice front along the floating tongue since early 2020, but diminishes before the grounding line is reached. Consistently, No ...o significant temporal changes...ariability in surface structure or ice flow speed are closer to the grounded ice. Our upper limit numerical simulations for a 400-year period are consistent with noticeable grounding line retreat in the Denman Glacier in the next two centuries if all floating ice were lost, before stabilising again in the third century from now. This equates to around 6 cm of sea level rise, a small contribution when compared to other areas of East Antarctica expected to change over the same time frame...It is clear that current knowledge is insufficient to explain the observed spatial and temporal chang... [6]

**Deleted:** Queen Mary and Knox coasts

numerical model predictions. With access to these remote coastal regions a major challenge, coordinated internationally collaborative efforts are required to quantify how much the [Shackleton](#) region is likely to contribute to sea level rise in the coming centuries.

Deleted: Queen Mary and Knox coastal

Deleted: ¶

## 1 Introduction

The East Antarctic Ice Sheet (EAIS) has historically been perceived as the stable sector of Antarctica (Silvano et al., 2016); however, it has now emerged that the Aurora and Wilkes subglacial basins of the EAIS have been contributing to sea level rise since the 1980s, with Aurora contributing 1.9 mm and Wilkes 0.6 mm (Rignot et al., 2019). Akin to large areas of the WAIS, these basins are grounded deep below sea level (Morlighem et al., 2020), and current estimates suggest that the sea level rise equivalent of the marine-based portion of the EAIS alone is five times larger than that of the marine-based portion of the WAIS (Morlighem et al., 2020). The EAIS is accordingly attracting increasing scientific attention, particularly in relation to whether climate and ocean warming could trigger substantial changes to the ice sheet, and the key timescales involved.

Deleted: ¶

Deleted: The health of the West Antarctic Ice Sheet (WAIS) has attracted much scientific scrutiny in recent decades but there has been less focus on the

Deleted: where

Deleted: the consensus was one of relative

Deleted: ility

Deleted: . H

Deleted: sea level rise

Deleted: S

The Shackleton system flows from a major drainage basin at the EAIS margin, located at the intersection of the Queen Mary and Knox coasts (Fig. 1a), including major outlet glaciers such as Denman, Scott, Northcliffe, Roscoe and Apfel. The floating component of the system is comprised of the Shackleton Ice Shelf together with the distinctive tongues of Denman, Scott and Roscoe, and an area of fast ice to the west of the Denman tongue (Fig. 1b). The Shackleton system is fed by one of the largest drainage basins in East Antarctica and is thought to connect to the western portion of the Aurora subglacial basin via the Knox Basin (Fig. 1a). The Denman Glacier alone is estimated to hold an equivalent of 1.5 m of sea level rise equivalent ice mass (Morlighem et al., 2020).

Deleted: ). It is supplied by several

Deleted: , including

Deleted: floating

Deleted: floating

Deleted: It is

Deleted: , located close to the margin of the continental shelf,

Deleted: thought

Despite the lack of an embayment and with the exception of localised fluctuations in ice flow, the Shackleton system has so far shown few signs of major dynamic change, with its flow restrained by islands, ice rises, and ice rumpled (Stephenson et al., 1989; Young, 1989). Analysis of Envisat data indicated that the Denman Glacier was thinning by 0.4 m year<sup>-1</sup> upstream of its grounding line between 2002 and 2010 (Flament and Rémy, 2012), and a 5.4 ± 0.3 km grounding line retreat was detected between 1996 and 2017–2018 (Brancato et al., 2020). Ice velocity data from the region are sparse before the late 2000s, but recent work identified an increase in ice velocity of the Denman Glacier of 16 % since the 1970s (Rignot et al., 2019), with an increase of 11 ± 5 % just upstream of the Denman grounding line between 1972–74 and 1989 and a more recent decrease of acceleration rate to 3 ± 2 % between 1989 and 2007–08 (Miles et al., 2021, their Fig. 3c).

Deleted: short-term

Deleted: g

Deleted: above

The discovery that the deepest sub-glacial trough in Antarctica (>3500 m below sea level) lies beneath the Denman Glacier, with a gentle and slightly retrograde bed slope close to the grounding line (Morlighem et al., 2020), has prompted suggestions that the system may be vulnerable to marine ice sheet instability, potentially triggered by high basal melt rates in the ocean cavity just offshore the grounding line (Brancato et al., 2020; Morlighem et al., 2020; Rignot et al., 2019). Meltwater

255 production from basal melt of the Shackleton system (73 Gt year<sup>-1</sup>) between 2003 and 2008 rivalled that from Thwaites (98 Gt  
year<sup>-1</sup>) (Rignot et al., 2013). Satellite derived basal melt rates between 2010 and 2018 revealed high but localised melt rates of  
> 50 m year<sup>-1</sup> close to the Denman grounding line (Liang et al., 2021), on par with basal melt rates in the Bellingshausen and  
Amundsen Sea (Adusumilli et al., 2020). These high basal melt rates have speculatively been linked to a strong bottom-  
intensified intrusion of modified CDW (mCDW) beneath fast ice south of the continental shelf break off the Sabrina Coast, at  
118° E (Williams et al., 2011). Such intrusions could facilitate persistent mCDW and associated ocean heat flux to this region  
260 of the continental shelf, which could expose the deep grounding line of the Shackleton system, particularly the Denman Glacier,  
to temperatures more than 3°C above the melting point (Rignot et al., 2019). Knowledge of the CDW in East Antarctica is still  
underdeveloped, however, and away from the grounding line, much of the floating ice across the system is observed to have  
little to no basal melt (Adusumilli et al., 2020; Liang et al., 2021). Refreezing on the order of 0.5 m year<sup>-1</sup> is observed at the  
Denman-Scott ground shear margin and 0.3 m year<sup>-1</sup> along the Denman-Shackleton floating shear margin (Adusumilli et al.,  
265 2020).

Despite increased scientific scrutiny in recent years (Arthur et al., 2020; Brancato et al., 2020; Miles et al., 2021; Morlighem  
et al., 2020; Rignot et al., 2019; Stokes et al., 2019), existing data and knowledge are still insufficient to predict the future  
evolution of the Shackleton system with confidence. Aside from incomplete understanding of the dynamic controls on Denman  
270 Glacier flow and Shackleton Ice Shelf stability, almost nothing is known about the adjacent Scott, Northcliffe, Roscoe and  
Apfel glaciers or their shear margins. Here we place the previously reported dynamic changes in the Denman Glacier into the  
wider regional context of the Shackleton Ice Shelf system. We do so by presenting an improved biannual temporal frequency  
of observations in the last eight years (2014-22), integrating airborne radar data, new satellite observations of ice structure,  
changes in ice front position and ice-flow velocities, with known geometrical and glaciological constraints.

## 275 2 Methods

### 2.1 Structure and feature mapping from optical and SAR imagery

Surface structures and features of the Queen Mary and Knox coasts were mapped from satellite imagery using standard GIS  
techniques (following Glasser et al. (2009)). Structural features have been mapped every 6 months from February 2015 to  
February 2022 using freely available datasets from Landsat 8 OLI and Sentinel 2A and 2B, where cloud cover is <15%, in  
280 combination with Sentinel 1A and 1B GRD to improve spatial and temporal coverage. To include multi-decadal changes in  
the extent and structure of the whole system, we used several different datasets from three time periods, only choosing the  
datasets that covered the entire area of interest. These include the declassified ARGON KH-5 images acquired 16<sup>th</sup> May 1962,  
Landsat 1 MMS acquired 27<sup>th</sup> February 1974, Landsat 5 TM acquired between 10<sup>th</sup> and 12<sup>th</sup> February 1991 and the MODIS  
Mosaic of Antarctica (MOA) image map, a composite of 259 swaths of both Aqua and Terra MODIS images acquired between  
285 01 Nov 2008 and 28 Feb 2009 (Scambos et al., 2007). Datasets were registered to the Sentinel-2 imagery as required.

Deleted: from

Deleted: /

Deleted:

Formatted: Superscript

Deleted: and s

Deleted: 6

Deleted: patchy

Deleted: f

Deleted: ice shelf

Deleted: A satisfactory explanation for the inferred high basal melt rates at the Denman Glacier grounding line is therefore still elusive. Melt rates could potentially be enhanced by vigorous channelized discharge of subglacial meltwater across the grounding line, by analogy with the nearby Totten Glacier (Dow et al., 2020).

Deleted: ¶

Deleted: D

Formatted: Normal, Left, Line spacing: single

Deleted: poor

Deleted: in the Queen Mary and Knox coasts

Deleted: observed

Deleted: in the Shackleton system

Deleted: Queen Mary and Knox coasts

Deleted: ,

Deleted: with

Deleted: seven

Deleted: 21

Deleted: ). We

Deleted: e

Deleted: We then use the BISICLES ice sheet model to assess the sensitivity and simulate the response times of the Queen Mary and Knox coasts to hypothetical disintegration of its floating ice areas in response to coupled ocean and atmospheric forcing.

Deleted: 2021

Deleted: (all downloaded from <https://earthexplorer.usgs.gov/>)

Deleted: (all downloaded from <https://scihub.copernicus.eu/dhus/#/home>), ...

Deleted: (all downloaded from <https://scihub.copernicus.eu/dhus/#/home>) ...

Deleted: (downloaded from <https://earthexplorer.usgs.gov/>)

Deleted: the

Deleted: (downloaded from <https://earthexplorer.usgs.gov/>)

Formatted: Superscript

Formatted: Superscript

325

Mapped features included, where visible, the ice-shelf or floating-glacier edges, rifts, crevasses and crevasse traces and longitudinal surface features following the methodology of Glasser et al. (2009). Interpretation of the optical imagery was performed using multiple band combinations to provide natural colour (Landsat-1 MSS bands 7-4-3, Landsat-5 TM bands 5-2-1 and Sentinel-2 bands 4-3-2) and for all imagery standard enhancement procedures (contrast stretching and histogram equalisation) were used to improve the contrast across features. The spatial resolution of the data sets varies from 10 m to 150 m and is thus a limitation on the minimum size and accuracy of the features mapped in each data set.

- Deleted: (
- Deleted: )
- Deleted: ;
- Deleted: (
- Deleted: )

330

## 2.2 Feature tracking from Sentinel-1

Glacier surface velocities were derived using feature tracking between pairs of synthetic aperture radar (SAR) images acquired by the Sentinel-1 satellite. Using the standard Gamma software and following commonly adopted methods, feature tracking uses cross-correlation to find the displacement of surface features between pairs of images, which are then converted to velocities using the time delay between those images (Luckman et al., 2007). We use image patch sizes of ~ 1 km in ground range, and sample at ~ 100 m in range and azimuth. Where the time-delay between images is sufficiently short, and surface change is minimized (for instance by very cold temperatures), trackable surface features include fine-scale coherent phase patterns (speckle) and the quality of the derived velocity map is maximised. We applied feature tracking to many image pairs and selected the best velocity map in terms of minimum noise and maximum coverage of high-quality matches for each year to provide mean annual velocity maps, including ice flow direction. We then produced percentage difference maps, scaled between +/- 10% but excluding data where the mean velocities are less than 0.2 m/day as uncertainties in velocity magnitude are around 0.2 m day<sup>-1</sup> (Benn et al., 2019). This approach allows us to optimize the quality of the surface strain map derived from the surface velocity.

Deleted: (all downloaded from <https://scihub.copernicus.eu/dhus/#/home>). F

335

Deleted: d

Deleted: ,

Deleted: d

340

Deleted: z

Formatted: Font: (Default) Times New Roman, 10 pt

Formatted: Font: (Default) Times New Roman, 10 pt

Deleted: U

Deleted: wed

Deleted: The image pair chosen was 18<sup>th</sup> to 24<sup>th</sup> November 2017 (6-day repeat between Sentinel-1B and Sentinel-1A).

345

Formatted: Font: Bold

Formatted: Font: Bold

## 2.3 Ice penetrating radar

The ice-penetrating radar data presented here were acquired on two survey flights using the Snow Eagle 601 BT-67 aircraft (Cui et al., 2018) flown on 19 and 20 December 2018. The data were acquired using a radar system that is functionally equivalent to the High Capability Airborne Radar Sounder that has been described in the literature (Peters et al., 2007) and used in numerous studies of both grounded (e.g. Young et al., 2011) and floating ice properties and grounding zones (e.g. Greenbaum et al., 2015). The images presented in this manuscript reflect a postprocessing sequence that coherently adds 10 raw radar records at a time to increase signal to noise, applies matched filtering to account for the chirped transmit pulse, then incoherently stacks the resulting complex valued radar traces five times to suppress speckle noise. The ice bottom elevation data were computed using a semiautomatic approach involving manual localization above and below horizons of interest (the ice surface and ice bottom interfaces in this instance).

Deleted: (

355

Formatted: Font: Bold

### 3 Results

#### 3.1 Ice front positions

375 Between 1962 and 2022, the shelf's central front advanced a total of 18 km with no obvious change in rate of advance (Fig. 2a). Calving occurred from the western side of the ice front in 1991, and a portion of the calved ice has since remained grounded just offshore of it (Fig. 2a). Between 2015 and 2022, the front then advanced steadily by  $\sim 0.3 \text{ km year}^{-1}$  while the Denman Glacier's ice front advanced at a rate of  $1.8 \text{ km year}^{-1}$  over the same time frame, with a uniform pattern of advance and no seasonal variability in advance rate observed (Fig. 2b). An iceberg from a calving event on the Denman Glacier, hypothesized to have occurred in the late 1940s ( $> 70 \text{ km}$  in length; Miles et al., 2021) is visible in 1962, roughly  $100 \text{ km}$  offshore the ice front (Fig. 2a). The Denman ice front position retreated in 1984 due to another major calving event ( $54 \text{ km}$  in length; Miles et al., 2021). By 1991 the floating margin was still located  $10\text{-}15 \text{ km}$  south of the 1962 position but has since advanced  $\sim 63 \text{ km}$  (Fig. 2a). The floating ice front of Scott Glacier has experienced more variability than that of Denman or Shackleton (Fig. 2a). Between 2015 and 2019, the front advanced at a steady rate of  $\sim 0.75 \text{ km year}^{-1}$  (Fig. 3a). Since early 2020, small scale calving has caused the ice front of the eastern half of the glacier to retreat  $\sim 5 \text{ km}$  further south of the 2015 front (Fig. 3b-d). In early 2022, the western side of the Scott Glacier ice front was in a similar position to that of 1962 but the whole ice front was  $\sim 10 \text{ km}$  further south in 2009 (Fig. 2a, 3) and in April 2022, a section  $> 25 \text{ km}$  long calved from the western side of Scott (Fig. 4c).

#### 3.2 Ice structure

390 Two major rift systems dominate on the Shackleton Ice Shelf, both of which extend westwards from its eastern lateral margin (labelled '1' and '2' in Fig. 1b). This margin is bordered to the east by a region of heavily fractured ice,  $\sim 2,300 \text{ km}^2$  in size (Fig. 1b), held in place by fast ice and  $\sim 150 \text{ m}$  thinner than the adjacent ice shelf body (Fretwell et al., 2013). System 1 is a maximum of  $\sim 15 \text{ km}$  wide at the eastern margin and extends over  $40 \text{ km}$  into the ice shelf, narrowing and eventually terminating at a spatially extensive suture zone that originates in the leeside cavity of Masson Island (Fig. 1b & 2a). A subsidiary rift branches off to the north and connects with the ice shelf front (Fig. 2a). The geometry of system 1 has not changed significantly since 1962, although its width increased by  $\sim 5.3 \text{ km}$  between 1962 and 1991 (Fig. 2a) and in 1962, there was no clear connection between the infant subsidiary rift and a front-parallel rift, visible by 1991 (Fig. 2a). System 2 is a maximum of  $\sim 5 \text{ km}$  wide at the eastern margin and extends into the shelf for  $16.5 \text{ km}$ , before branching into two rifts that trend in opposing directions,  $\sim 14 \text{ km}$  and  $\sim 21 \text{ km}$  in length respectively (Fig. 1b & 2a). System 2 changed more substantially than system 1, branching towards the grounding line and lengthening by  $3.8 \text{ km}$  between 2015 and 2022. In 1962 the rift is only visible as a crack, opening to a rift  $2.3 \text{ km}$  wide by 1991 and at the eastern edge,  $4.5 \text{ km}$  wide by 2017 (Fig. 1b & 2a). Between 1991 and 2015 its southwestern branch increased in length from  $\sim 10 \text{ km}$  to  $\sim 16 \text{ km}$  and in width by  $\sim 1 \text{ km}$  at the ice margin (Fig. 1b & 2a). The northern crack increased in length from  $\sim 13 \text{ km}$  to  $\sim 16 \text{ km}$  over the same time-period. Both

Deleted: 2.3 BISICLES ice flow model

We used the BISICLES ice flow model to investigate the response of the Queen Mary and Knox coasts to hypothetical sustained disintegration of floating ice, while surface mass balance remains at present day values. A similar investigation carried out for the whole of Antarctica (Martin et al., 2019) was unable to comment on this region because the Bedmap2 bedrock (Fretwell et al., 2013) did not resolve the Denman trough. Here, we address that short coming by using ice thickness and bedrock elevation data from BedMachine v2 (Moriglighem et al., 2020), which includes a deep trough beneath Denman Glacier. The model simulates the flow of ice numerically, employing finite-volume discretizations of an ice thickness transport equation

$$\frac{\partial h}{\partial t} + \nabla \cdot (uh) = a - m \quad (1)$$

and a two-dimensional vertically integrated stress balance equation,

$$\nabla \cdot [h\phi\mu(2\epsilon + 2tr(\epsilon))] - \tau_b = \rho gh\nabla s$$

Deleted: Between 2015 and 2021 the floating ice front of th...

Deleted: 3

Deleted: Between 1962 and 2021 the shelf's central front ad...

Deleted: between 2015 and 2021

Deleted: 3

Deleted: 3

Deleted: 61

Deleted: 3

Deleted: Remarkably, t

Deleted: 3

Deleted: 4

Deleted: 4

Deleted: T

Deleted: i

Deleted: in 2021 to that

Deleted: 3

Deleted: 4c

Deleted: .

Deleted: 3

Deleted: 3

Deleted: 3

Deleted: 3

Deleted: 3

Deleted: 3

Deleted: 2021

Deleted: 3

Deleted: 3a

Deleted: 3

systems advected with ice flow towards the ice front between 2015 and 2022, with no significant changes in geometry (Fig. 2a).

Deleted: 2021

Deleted: 3

The surface of the Denman Glacier is heavily featured with a combination of crevasses, flow lines and channel-like features (Fig. 1b). A number of small rifts (< 6km long) are evident along the western margin, separated by fast ice from Shackleton Ice Shelf and there is no identifiable change on the length or position of these rifts relative to the ice front between 2015 and 2022 (Fig. 2b). The floating portion of Scott Glacier is dominated by a series of rifts striking perpendicular to the flow direction (Fig. 4). The rifts initiate approximately 20 km down glacier of the grounding line and widen to ~ 2.5 km as they flow around the Taylor Islands. Between 2015 and 2022 the up-flow (southern) rift widens at a rate of ~ 200 m year<sup>-1</sup> (Fig. 4a -labelled 1), while the down-flow rift narrows at a rate of ~ 100 m year<sup>-1</sup> (Fig. 4a -labelled 2). The rift formation, widening and narrowing process is evident from 1962 through to 2009 (Fig. 4b). A rift on the eastern side of Scott Glacier, initiated from the eastern Scott shear margin, has increased in length toward Chugunov Island by ~ 5 km between February 2021 and June 2022 (Fig 4c -labelled 3). There is little observable change in Roscoe Glacier with the exception of a rift opening in the vicinity of the margin with Shackleton Ice Shelf (Fig 5). In 2022 the rift is 15 km long and 2 km wide at the widest point and extends to within 3.2 km of the ice front, a significant increase in dimensions of 5.3 km and 0.35 km, observable in 2015 when the feature terminated 8.5 km from the ice front (Fig 5).

Deleted: g

Deleted: 2021

Deleted: 3

Deleted: 1

Deleted: 6

Deleted: )

Deleted: 2021

Deleted: .

Deleted: -

Deleted: (northern)

Deleted: .

Deleted: -

Deleted: Fig. 5a

Deleted: 5b

Deleted: western

Deleted: initiating close to the margin with Chugunov Island, now connects with an opening rift at the ice front, detaching a portion of the front of Scott, > 24 km in length (Fig. 5c

Deleted: 6

Deleted: 2021

Deleted: 6

Deleted: there are some changes

Deleted: between

Deleted: and

Deleted: 2021

Deleted: 7

Deleted: 7a

Deleted: 7

Deleted: 2021

Deleted: 7c

Formatted: Font: 10 pt

Formatted: Font: 10 pt

Formatted: Font: 10 pt

Formatted: Font: 10 pt

Across the whole system, small-scale changes have been observed in the shear margins separating the various inlet glaciers and along the main body of the Shackleton Ice Shelf. Between 2015 and 2022, small changes are observable in the floating shear margins to the east (abutting Apfel Glacier and Taylor Islands) and west (abutting Denman Glacier) of Scott Glacier (Fig. 6). The eastern margin appears as a series of small rifts and crevasses, largely perpendicular to ice flow (Fig 6a-b). Over the 7-year period there has been lengthening of the features into the ice to both the east and the west of the eastern margin, as well as opening of existing features (Fig. 6). The western shear margin of Scott Glacier is more clearly defined and has been widening into Denman Glacier in the vicinity of Chugunov Island (Miles et al., 2021). In 2015 this margin is relatively straight, in line with the floating margin of Denman and ~ 1.3 km wide. Remarkably, the shear margin appears to bulge progressively into Denman Glacier and is double the width by 2022 as compared with 2015 (Fig 6c-d).

The ICECAP airborne radar lines flown in December 2016 provide information about the thickness and ice structure through the floating ice. The western side of Shackleton thins from ~300 m thick, closer to the grounding line to ~150 m thick close to the Denman shear margin (fig. 7a), with a smooth, clearly defined ice base (Fig 7b). A clear near surface reflector is found in the Shackleton region in all 6 radar lines, ~ 50 below the main surface reflector, at ~0 m asl in elevation (Fig. 7b). The Denman tongue appears split longitudinally into two sections with very different ice thicknesses, with the portion adjacent to Shackleton ~ 130-150 m thick and originating from Northliff Glacier (Fig. 7a). The eastern side of Denman ranges from ~ 300 m to >500 m thick towards the central flowline (Fig. 7a), with the thickest parts of the tongue following the longitudinal

595 features visible at the surface (Fig. 7a). In all 6 radar lines the Denman region shows significant surface and basal roughness but is also consistently noisy (Fig. 7a). The Scott tongue has less variation in thickness across the width but thins from ~370 m thick in the vicinity of the first rift to ~150 m thick close to the ice front (Fig. 7a). The radar lines which extend into the region east of the Scott shear margin, towards the Taylor Islands and Mill Island appears dimmer, and the reflectors muted (Fig. 7b).

### 600 3.3 Ice flow speed

Mean ice speed derived at annual temporal frequency from Sentinel-1 data varies across the Shackleton System. In 2021, ice speed ranges from ~0.2 m day<sup>-1</sup> in the area between the grounding line and Masson Island on the Shackleton Ice Shelf to ~5 m day<sup>-1</sup> on the floating tongue of Denman Glacier (Fig. 8a). Surface ice speeds observed along Roscoe and Scott glaciers reach 1-2 m day<sup>-1</sup> and 2-3 m day<sup>-1</sup>, respectively. Recent changes in ice speed, derived by differencing the mean speed across the whole system between 2021 and 2018, are confined to the seaward ~60 km of the floating tongue of Scott Glacier and the Shackleton Ice Shelf (Fig. 8b). On the floating portion of Scott Glacier increases of >10% occur across the outer 50 km (Fig. 8b). The western side of the Shackleton ice shelf, including the fast ice to the western side, appears to have decelerated over the same time period, where a change of between -4% and -6% is observed (Fig. 8b). There is some evidence of deceleration on the eastern side of the ice shelf, although the signal is unclear with values ranging between +/- 5%. Annual ice speed percentage differences illustrate the increase in ice speed on the eastern flank of the ice front of Scott Glacier between 2017 and 2018 (Fig. 9a), which then appears to decelerate between 2018 and 2019, when a 4% increase in the ice speed of the western flank of the ice front is observed (Fig. 9b). The increase in speed continues through 2019-2020 with a 10% acceleration from the ice front up to 45 km upstream and across the entire ice tongue width (Fig. 9c). The increase extends a further 15 km in the up-flow direction between 2020 and 2021 (Fig. 9d). There is more spatial variability in the annual speed percentage differences across the Shackleton Ice Shelf. The overall trend between 2018 and 2021 appears to be deceleration but there are small regions of acceleration and much of the variability is within the uncertainty bounds, thus complicating interpretation (Fig. 8b).

Ice speed extracted from Sentinel-1 provides a timeseries between 2017-2021, which we extend back to 2002 using MEaSURES (Mouginot et al., 2012, 2019; Rignot et al., 2011) and ITS LIVE (Gardner et al., 2018, 2021) in locations where available to highlight variability through time across the system (Fig. 8 and 10). Point locations on Shackleton Ice Shelf vary between ~0.2 m day<sup>-1</sup> at the grounding line (point 3 and 4 in Fig. 8b) and ~1 m day<sup>-1</sup> towards the front of the floating ice (point 2 in Fig. 8b), with no consistent temporal trends (Fig. 10a). Denman Glacier exhibits higher speeds, from <2 m day<sup>-1</sup> upstream of the grounding line (point 5 in Fig. 8b) to ~5 m day<sup>-1</sup> on the floating tongue (point 9 in Fig. 8b) but speeds remain constant through time at each point location (Fig. 10b). Scott Glacier has a similar spatial pattern with speeds increasing from ~1.2 m day<sup>-1</sup> at the grounding line (point 10 in Fig. 8b) to >4 m day<sup>-1</sup> close to the floating ice front (point 13 in Fig. 8b; Fig. 10c). There is no observable change in speed within 10 km of the grounding line of Scott Glacier (points 10 and 11 in Fig. 8b;

Formatted ... [10]

Deleted: Tyler

Formatted ... [11]

Deleted: flow...speed derived at bi...annual temporal frequency from Sentinel-1 data between 2017 and 2021 ...aries across the Queen Mary and Knox coasts...hackleton System. It ... [12]

Deleted: it

Deleted: 8a

Deleted: Roscoe Glacier shows speeds of 1-2 m day<sup>-1</sup>, higher than the surrounding ice shelf and the floating portion of Scott Glacier reaches 2-3 m day<sup>-1</sup>.

Deleted: 0... and 2019 ... [13]

Deleted: lower ... seaward ~60 km of the floating tongue of Scott Glacier (Fig. 8b) ... [14]

Deleted: I...reases of >0.2 m day<sup>-1</sup>...0% occur across the outer 50 km, decreasing to ~0.08 m day<sup>-1</sup> close to the large rift adjacent to the Taylor Islands ... Fig. 8b...b). The western side of the Shackleton ice shelf, including the fast ice to the western side, appears to have decelerated over the same time period, where a change of between -4% and -6% is observed (Fig. 8b) No acceleration (or deceleration) is observed elsewhere in the system (Fig. 8b)... There is some evidence of deceleration on the eastern of the ice shelf, although the signal is unclear with values ranging between +/- 5%. ... [15]

Deleted: whole width of Scott...ntire ice tongue width (Fig. 9c). The increase extends a further 15 km in the up-flow direction between 2020 and 2021 (Fig. 9d). There is more spatial variability in the annual speed percentage differences across the Shackleton Ice Shelf... The overall trend between 2018 and 2021 appears to be deceleration but there are small pockets...egions of acceleration and much of the variability is within the uncertainty bounds, making interpretation problematic ... [16]

Deleted: flow

Deleted: ed...a timeseries between 2017-2021, extended ... [17]

Deleted: easures

Deleted: 19

Field Code Changed

Deleted: it is

Deleted: (Rignot et al., 2017)... ... [18]

Deleted: ...highlighting ... [19]

Deleted: s... 9 ... and 10...0). Point locations on Shackleton Ice Shelf vary between ~0.2 m day<sup>-1</sup> at the grounding line (point 3 and 4 in Fig. 8b) and ~1 m day<sup>-1</sup> towards the front of the floating ice (point 2 in Fig. 8b), with no consistent temporal trends (Fig. 9a...0a). Denman Glacier exhibits higher speeds, from <2 m/ ... [20]

Formatted: Superscript

Deleted: 9...). Scott Glacier has a similar spatial pattern with speeds increasing from ~1.2 m day<sup>-1</sup> at the grounding line (p... [21]

Deleted: >...0 km downstream ... [22]

760 [Fig. 10c](#)). However, the [downstream](#) 30 km of the floating ice tongue show significant acceleration from the beginning of 2020 through to May 2021 ([points 12 and 13 in Fig. 8b](#); [Fig. 9c](#)). Over the 17-month period, ice speeds increase ~ 30 % to 2.5 m day<sup>-1</sup> 30 km from the ice front ([point 12 in Fig. 8b](#)) and ~ 40 % to 3.2 m day<sup>-1</sup> close to the front ([point 13 in Fig. 8b](#); [Fig. 10c](#)). Roscoe Glacier has similar [ice speed](#) spatial patterns to both Shackleton and Denman, with slower speeds of ~ 0.4 m day<sup>-1</sup> at the grounding line ([point 14 in Fig. 8b](#)), increasing to ~1.2 m day<sup>-1</sup> close to the floating ice front ([point 16 in Fig. 8b](#)) and no significant change in speed through time ([Fig. 10d](#)).

765 The magnitude of the principal strain rate, derived from mean velocity maps, highlights the shear margins of the Denman Glacier and those of Scott and Roscoe [glaciers](#) ([Fig. 11](#)), as well as [pinning points](#) of the Shackleton Ice Shelf ([Fig. 11](#)). [Pinning points](#) have previously been identified at the front of the Roscoe - Shackleton shear margin ([label-a in Fig. 10](#)) and upstream of rift 2 on the Shackleton Ice Shelf ([label-b in Fig. 11](#), [Fürst et al., 2015](#)). There is evidence of two additional [pinning points](#), [Chugunov Island](#) at the front of the Denman-Scott shear margin ([label-c in Fig. 11](#)) and at the ice margin of Shackleton Ice Shelf ([label-d in Fig. 10](#)). The latter coincides with a [local topographic high in ocean bathymetry](#) ([Arndt et al., 2013](#)).

#### 4 Discussion

775 Over the ~ 60-year period of observation, the [Shackleton Ice Shelf system](#) has [undergone observable variability in velocity and structure, but there is no sustained longer-term change](#). More frequent satellite observations in recent years have not revealed any distinct [seasonal or annual cycles](#) of change in the system. With prominent suture zones and pinning points as likely agents of stability ([Kulesa et al., 2014, 2019](#)), the front of the Shackleton [Ice Shelf](#) is only slowly advancing and little change in the geometry of the main surface features occurs. [Throughout the period of observation there is little evidence of an increase in surface melt or ponding on Shackleton](#) ([Arthur et al., 2020](#)) but the persistent reflector at ~0 m asl in the airborne [radar data over Shackleton](#) ([Fig. 7b](#)) could be a result of strong melting and refreezing events observed on ice shelves elsewhere ([Kuipers Munneke et al., 2017](#)). [These would lead to enhanced firm air depletion and are hypothesised to be a precursor to ice shelf collapse](#) ([Kuipers Munneke et al., 2014](#)). However, [an equally plausible interpretation of the bright reflector could be brine infiltration of the firm layer as this region lies within a zone thought to be susceptible to brine infiltration](#) ([Cook et al., 2018](#)). [Brine has been detected in firm cores from a number of Antarctic ice shelves](#), ([Heine, 1968](#); [Kovacs et al., 1982](#); [Risk and Hochstein, 1967](#); [Thomas, 1975](#)) and observed as a bright reflector close to sea level in radar data on the [McMurdo](#), ([Campbell et al., 2017](#); [Grima et al., 2016](#)), [Wilkins](#) ([Vaughan et al., 1993](#)), [Larsen](#) ([Smith and Evans, 1972](#)), [Brunt](#), ([Walford, 1964](#)), and [Ross ice shelves](#), ([Neal, 1979](#)). [Although both suggestions are plausible, at this location, further work is needed to identify the cause of the reflector more conclusively](#).

790 [Flow speed of the Shackleton ice shelf](#) is regulated by the extensive suture zone downstream of Masson Island ([Fig 1b, 2a](#)) that arrests the two large rift systems, and by pinning points at the front of the Roscoe-Shackleton shear margin, on the western side of the ice shelf and to the inland side of the large rifts ([Fig. 11](#)). [The lack of significant rift propagation on the main body](#)

**Deleted:** Speeds ~ 10 km either side of the grounding line show no change through time however, the outer (... [23])

**Deleted:**

**Deleted:** 9c...0c). Roscoe Glacier has similar ice speed spatial patterns to both Shackleton and Denman, with slower speeds of ~ 0.4 m day<sup>-1</sup> at the grounding line ([point 14 in Fig. 8b](#)), increasing to ~1.2 m day<sup>-1</sup> close to the floating ice front ([point 16 in Fig. 8b](#)) and no significant change in speed through time ([Fig. 9d](#)) (... [24])

**Deleted:** G

**Deleted:** 10...1), as well as pinning points of the Shackleton Ice Shelf ([Fig. 10...1](#)). Pinning points have previously been identified at the front of the Roscoe - Shackleton shear margin ([label-a in Fig. 10...0](#)) and upstream of rift 2 on the Shackleton Ice Shelf ([label-b in Fig. 10](#)) (... [25])

**Deleted:** (

**Field Code Changed**

**Deleted:** (c)...in [Fig. 10...1](#)) and at the ice margin of Shackleton Ice Shelf ([label-d in Fig. 10...0](#)). The latter coincides with a rise in the ocean floor...ocal topographic high in ocean bathymetry ([Arndt et al., 2013](#)). ¶ (... [26])

**Deleted:** Figure 11 shows the results of the model calibration over subset of the domain including the majority of the fast flow. Following the optimization of Eqn. (5), model and observed speeds have an r.m.s. difference of 44 m a<sup>-1</sup> over the region shown, compared to an r.m.s. model speed of 380 m a<sup>-1</sup>. The remainder of the domain is dominated by slow flow in both model and observations. Basal traction over the region varies by around one order of magnitude from ~10 kPa to ~100 kPa, with stripes of soft and hard bed appearing both in the glacier trunks and outside. The stiffness factor  $\phi$  appears similar to other BICISLES optimizations, with weak shear margins apparent in both ice stream and ice shelf regions. The future simulation shows the response of the system to hypothetical rapid, immediate, and sustained disintegration of the floating ice. A notable and rapid retreat of Denman Glacier occurs after 2150, but otherwise the overall dynamic response is modest ([Fig. 12](#)). Between 2010 and 2110, the loss of essentially all floating ice in the Denman Glacier shelf leads to around 20 km of grounding line retreat of the Denman and neighbouring Scott glaciers ([Fig. 12](#)). At the same time, flow across the grounding line discharges 80-100 Gt year<sup>-1</sup> ice volume above flotation ([Fig. 13](#)). In the following century, the grounding line in the Denman trough retreats by around 100 km over the region of lowest elevation ([Fig. 12](#)), while discharge increases to more than 200 Gt year<sup>-1</sup> volume above flotation in 2150 ([Fig. 13](#)). This period of rapid change is only temporary on a centennial scale with a cumulative sea level rise contribution of ~ 6 cm, and by the following century ice grounding line retreat has all but ceased (... [27])

**Deleted:** Queen Mary and Knox coasts...hackleton Ice Shelf system have...not changed significantly...ndergone observable variability in velocity and structure, but there is no sustained (... [28])

**Field Code Changed**

**Formatted**

**Deleted:** The f...ow speed of the Shackleton ice shelf is regulated by the extensive suture zone downstream of Masson Island ([Fig 1b, 23...](#)) that arrests the two large rift systems, and by pinning (... [30])

**Formatted:** Font: Not Italic



955 of Shackleton Ice Shelf appears directly related to the Masson Island suture zone. Indeed, there is growing recognition that the softer marine ice present in suture zones inhibits the growth of large-scale fractures, acting to stabilise ice-shelves by reducing local stress intensities (Kulesa et al., 2014; Larour et al., 2021; McGrath et al., 2014). Suture zones are structurally and mechanically heterogeneous and therefore particularly susceptible to micro-crack formation ahead of the rift tip, reducing the stress intensity around the rift tip and potentially causing rifts to be halted by suture zones (Bassis et al., 2007; Kulesa et al., 2019). In addition, stress intensities around the rift tip are likely to be reduced because of sea-water softened suture-zone ice, relative to harder meteoric ice that is colder and contains less liquid seawater (Kulesa et al., 2019). While current observations suggest suture zones promote stability by halting rift propagation, a strong relationship between the thickness of ice mélange and the opening rate of the rifts has been observed, indicating that ice mélange thinning rather than ice shelf thinning can promote rift propagation (Larour et al., 2021). The warmer temperature and increased sea water content of the ice mélange suggests it may be more vulnerable to thinning due to future surface and basal melting than the surrounding meteoric ice, potentially affecting rates of rift opening and propagation (Kulesa et al., 2014; McGrath et al., 2014).

The Denman tongue is comprised of two distinct ice masses: heavily crevassed, thinner ice originating from Northcliff Glacier on the western side and significantly thicker, crevassed ice on the eastern side, originating from Denman Glacier (Fig. 7). The eastern side has distinctive longitudinal features that correspond to the thickest parts of the tongue (Fig. 7). Both sides of the Denman tongue exhibit significant basal roughness (Fig. 7), which has been cited to significantly influence heat and salt exchange at the ice-ocean interface (Watkins et al., 2021). An increase in ice flow speed was observed just upstream of the Denman Glacier grounding line between 1972-4 and 1989 and, to a lesser extent, through to 2008 (Miles et al., 2021, their Fig. 3c). Variability in ice flow speed then became insignificant through to 2016-17 (Miles et al., 2021, their Fig. 3c), a pattern that has continued since (Fig. 8b, 10b) and, accordingly, is not associated with change in the surface structure of the system (Fig. 2). Scott Glacier has received less attention until now, being thinner and slower than Denman, with an overall decrease in velocity observed between 1972-4 and 2016-7 (Miles et al., 2021). However, this part of the system is where we observe more recent change (Fig. 4, 6, 7, 8, 9, 10). Since early 2020, ice flow acceleration has been progressing from the calving front along the floating tongue of Scott Glacier and is particularly pronounced within the frontal ~ 60 km (Fig. 8b), where small-scale calving has been progressively observed (Fig. 4, 5c). The muted reflectors in the radar lines that extend past the eastern Scott shear margin (Fig. 7b) may indicate that the extremely high salt concentration found in the Mill Island ice core (Inoue et al., 2017) extends from Mill Island up-flow towards the grounding line (Fig. 7a). No changes in structure or ice flow speed are observed up flow of the large rift to the west of the Taylor Islands (Fig. 4c – labelled 1), and the acceleration does not currently appear to have any connection to the grounded ice (Fig. 8b, 10c). Surface meltwater features, reported to be frequent around the Scott and Apfel grounding lines, do not appear to be increasing in area or frequency between 2000 and 2020 (Arthur et al., 2020) and are unlikely to be contributing to the changes observed on Scott Glacier.

Deleted: .  
Deleted: with  
Deleted: ...implicatio  
Deleted: ns?  
Deleted: 1  
Deleted: 8  
Deleted: 9  
Deleted: we cannot identify any related  
Deleted: 3  
Deleted: more significant  
Deleted: since early 2020  
Deleted: 5  
Deleted: 7  
Deleted: 8  
Deleted: 9  
Deleted: )  
Deleted: 1  
Deleted: is  
Deleted: Scott Glacier and  
Deleted: 8  
Deleted: 5  
Deleted: 9  
Deleted: ¶  
The upper limit scenario of forcing in our BISICLES model runs suggests that noticeable grounding line retreat occurs in the Denman Glacier over the simulated 400-year time period, briefly doubling the discharge of mass above flotation to 200 Gt year<sup>-1</sup> around the year 2150, before stabilising again with discharge returning to around 100 Gt year<sup>-1</sup> (Fig. 13). With a cumulative contribution of ~ 6 cm to sea level rise the increased discharge is not insignificant, but small compared to possible contributions from other areas of East Antarctica over the same time frame (Martin et al., 2019). Our newly discovered and any previous reported changes in the Denman and Scott Glaciers are much smaller than those considered here as an upper limit of forcing in BISICLES. Any real future dynamic changes and contributions to sea level rise will therefore very likely be less than those illustrated here. ¶  
¶ One possible interpretation of the model output is that Queen Mary and Knox coasts are relatively stable and insensitive to reasonable forcing in next 400 years, and that ice loss from the Shackleton system poses no imminent threat to the Aurora and Wilkes subglacial basins. This interpretation is reinforced in that implied rates of basal melting of the Denman ice tongue, albeit high on a continental scale, are likely much lower than those required to precipitate full disintegration of the Denman Glacier floating tongue on the short timescales simulated here. However, our BISICLES simulation may suffer from poor boundary constraints due to unknown or poorly known subglacial substrate, basal hydrology, geothermal heat flux, ice properties, oceanographic conditions, and bathymetry. ¶

On the nearby Totten Glacier, inferences from combined geophysical exploration and numerical modelling are consistent with areas of high basal melt rate coinciding with significant grounding line retreat, possibly linked to channelized subglacial meltwater discharge (Dow et al., 2020). By analogy, the deep trough beneath the Denman Glacier is also likely to favour vigorous channelization of the subglacial meltwater system close to the grounding line. As freshwater outflow into the sub-ice shelf ocean cavity can locally enhance basal melt rates melting near the grounding line (Jenkins, 2011; Wei et al., 2020), the recently observed retreat of Denman Glacier towards the deepest continental trench on Earth could result from complex interplay between the ice, ocean, and subglacial environments. In addition, interaction of Denman Glacier with neighbouring Scott and Northcliff glaciers, as well as with the numerous surface features and pinning points highlighted in this work, could influence how this ice mass responds to future changes in forcing conditions. As this sector of Antarctica holds over 2 m of global sea level potential, it is critical that we continue to both support numerical modelling efforts of this region and monitor short- and long-term changes of the Shackleton system.

## 5 Conclusions

We conclude that over the 60-year period of observation, the Shackleton Ice Shelf system does not appear to have major, ongoing change, and higher frequency observations have not revealed any significant annual or sub-annual variations in ice flow. The velocity changes on the Denman Glacier recently described (Miles et al., 2021; Rignot et al., 2019) appear to be short-lived events focused on the glacier itself. We do observe more significant change in the Scott Glacier, with an acceleration in ice flow likely triggered by calving and progressing from the ice front along the floating tongue since early 2020. These short-term changes in the flow speed and structure of Scott Glacier have not yet had any noticeable impact on ice dynamics close to the grounding line; however, should the recent calving continue through the full length of the area experiencing an increase in speed, there may be changes in the buttressing for both the Scott and Denman glaciers. As such, it remains unclear whether the previously reported short-lived changes are just that, or whether they herald more significant future change. Given the potential vulnerability of the system to accelerating retreat, better data recording the glaciological, oceanographic, and geological conditions in the Shackleton Ice Shelf system are urgently required to improve the certainty of numerical model predictions that constrain the potential future sea level contribution from this dynamic sector of Antarctica.

## Acknowledgements

This project received grant funding from the Australian Government as part of the Antarctic Science Collaboration Initiative program, the AXA Research Council through an AXA Post-Doctoral Fellowship and The National Natural Science Foundation of China grant 41941007. J.S.G. acknowledges supported from NSF OPP-2114454 and NASA grant 80NSSC22K0387. L.M.J. and J.L.R. acknowledge support from Australian Antarctic Division project 4346 and the Antarctic Gateway Partnership (University of Tasmania, Australia). J.G. acknowledges support from the National Natural Science Foundation of China grant 41941007. We thank Gregory Ng for engineering support in the field and with radar data processing.

## Data availability

**Formatted:** Justified, Line spacing: 1.5 lines, Adjust space between Latin and Asian text, Adjust space between Asian text and numbers, Tab stops: Not at 0.99 cm + 1.98 cm + 2.96 cm + 3.95 cm + 4.94 cm + 5.93 cm + 6.91 cm + 7.9 cm + 8.89 cm + 9.88 cm + 10.86 cm + 11.85 cm

**Formatted:** Font: (Default) +Body (Times New Roman), 10 pt

**Formatted:** Font: (Default) +Body (Times New Roman), 10 pt

**Formatted:** Font: (Default) +Body (Times New Roman), 10 pt

**Formatted:** Font: (Default) +Body (Times New Roman), 10 pt

**Formatted:** Font: (Default) +Body (Times New Roman), 10 pt

**Deleted:** Basal water and ice sheet behaviour are also affected by geothermal heat flow. Regional values of ~ 55-85 mW m<sup>-2</sup> are interpreted from magnetic (Martos et al., 2017) and seismic (An et al., 2015) data, similar to the average global value of ~ 67 mW m<sup>-2</sup> for continental regions (Lucazeau, 2019). Multivariate analysis of Antarctic and global geophysical and geological datasets is consistent with elevated geothermal heat flow, > 70-80 mW m<sup>-2</sup>, west of the Denman region near the Gaussberg Volcano (Wilhelm II Coast) and in the Knox interior (Stål et al., 2021). These high heat flow anomalies remain poorly resolved but are likely driven by the geological evolution including volcanism, neotectonics and variation in crustal heat production, thermal conductivity and topography (Stål et al., 2021). The geometry and infill of the subglacial Knox Sedimentary Basin (Maritati et al., 2016) likely imparts impact (... [31])

**Deleted:** Queen Mary and Knox coasts

**Deleted:** d significantly

**Deleted:** red

**Deleted:** g

**Deleted:** G

**Deleted:** . Nonetheless, the BISICLES ice flow model provides us with initial insights into the extent to which reasonable upper (... [32])

**Deleted:** Queen Mary and Knox coasts

**Deleted:**

**Deleted:** . It remains unclear whether the previously reported short-lived changes are just that, or whether they herald more significant future change (... [33])

**Formatted:** Justified

**Deleted:** and

**Formatted:** Font: (Default) +Body (Times New Roman), 10 pt, Font colour: Text 1

**Formatted:** Font colour: Text 1

**Formatted:** Font: (Default) +Body (Times New Roman), 10 pt, Font colour: Text 1

**Deleted:** .

**Formatted:** Font: Bold

145 [All satellite imagery used in this work are freely available as follows; Landsat 8 OLI, 5 TM, and 1 \(all downloaded from https://earthexplorer.usgs.gov/\), MODIS Mosaic of Antarctica 2008-2009 \(downloaded from https://nsidc.org/data/nsidc-0593/versions/2\), Sentinel 2 A and B \(all downloaded from https://scihub.copernicus.eu/dhus/#/home\) Sentinel 1A and B GRD \(all downloaded from https://scihub.copernicus.eu/dhus/#/home\) and ARGON KH-5 \(downloaded from https://earthexplorer.usgs.gov/\).](https://earthexplorer.usgs.gov/)

## References

- 1150 Adusumilli, S., Fricker, H. A., Medley, B., Padman, L. and Siegfried, M. R.: Interannual variations in meltwater input to the Southern Ocean from Antarctic ice shelves, *Nat. Geosci.*, 13(9), 616–620, doi:10.1038/s41561-020-0616-z, 2020.
- Arndt, J. E., Schenke, H. W., Jakobsson, M., Nitsche, F., Buys, G., Goleby, B., Rebesco, M., Bohoyo, F., Hong, J. K., Black, J., Greku, R., Udintsev, G., Barrios, F., Reynoso-Peralta, W., Morishita, T. and Wigley, R.: The International Bathymetric Chart of the Southern Ocean (IBCSO) Version 1.0 - A new bathymetric compilation covering circum-Antarctic waters, *Geophys. Res. Lett.*, 40, 3111–3117, doi:doi: 10.1002/grl.50413, 2013.
- 1155 Arthur, J. F., Stokes, C. R., Jamieson, S. S. R., Rachel Carr, J. and Leeson, A. A.: Distribution and seasonal evolution of supraglacial lakes on Shackleton Ice Shelf, East Antarctica, *Cryosphere*, 14(11), 4103–4120, doi:10.5194/tc-14-4103-2020, 2020.
- Bassis, J. N., Fricker, H. A., Coleman, R., Bock, Y., Behrens, J., Darnell, D., Okal, M. and Minster, J. B.: Seismicity and deformation associated with ice-shelf rift propagation, *J. Glaciol.*, 53(183), 523–536, doi:10.3189/002214307784409207, 2007.
- Benn, D. I., Jones, R. L., Luckman, A., Fürst, J. J., Hewitt, I. and Sommer, C.: Mass and enthalpy budget evolution during the surge of a polythermal glacier: a test of theory, *J. Glaciol.*, 65(253), 717–731, doi:10.1017/JOG.2019.63, 2019.
- Brancato, V., Rignot, E., Milillo, P., Morlighem, M., Mouginot, J., An, L., Scheuchl, B., Jeong, S., Rizzoli, P., Bueso Bello, J. L. and Prats-Iraola, P.: Grounding Line Retreat of Denman Glacier, East Antarctica, Measured With COSMO-SkyMed Radar Interferometry Data, *Geophys. Res. Lett.*, 47(7), e2019GL086291, doi:10.1029/2019GL086291, 2020.
- Campbell, S., Courville, Z., Sinclair, S. and Wilner, J.: Brine, englacial structure and basal properties near the terminus of McMurdo Ice Shelf, Antarctica, *Ann. Glaciol.*, 58(74), 1–11, doi:10.1017/aog.2017.26, 2017.
- Cook, S., Galton-Fenzi, B. K., Ligtenberg, S. R. M. and Coleman, R.: Brief communication: Widespread potential for seawater infiltration on Antarctic ice shelves, *Cryosphere*, 12(12), 3853–3859, doi:10.5194/tc-12-3853-2018, 2018.
- 1170 Cui, X., Greenbaum, J. S., Beem, L. H., Guo, J., Ng, G., Li, L., Blankenship, D. and Sun, B.: The First Fixed-wing Aircraft for Chinese Antarctic Expeditions: Airframe, modifications, Scientific Instrumentation and Applications, *J. Environ. Eng. Geophys.*, 23(1), 1–13, doi:10.2113/JEEG23.1.1, 2018.
- Dow, C. F., McCormack, F. S., Young, D. A., Greenbaum, J. S., Roberts, J. L. and Blankenship, D. D.: Totten Glacier subglacial hydrology determined from geophysics and modeling, *Earth Planet. Sci. Lett.*, 531, 115961, doi:10.1016/j.epsl.2019.115961, 2020.
- 1175 Flament, T. and Rémy, F.: Dynamic thinning of Antarctic glaciers from along-track repeat radar altimetry, *J. Glaciol.*, 58(211),

Formatted: Font: Not Bold

Formatted: Font: Not Bold

Formatted: Font: Not Bold

Formatted: Font: Not Bold

Formatted: Line spacing: single

Formatted: Hyperlink, Font: Not Bold

Formatted: Font: Not Bold

Field Code Changed

Formatted: Font: Not Bold

Formatted: Hyperlink, Font: Not Bold

Formatted: Font: Not Bold

Formatted: Font: Not Bold

Field Code Changed

Formatted: Hyperlink, Font: Not Bold

Formatted: Font: Not Bold

Field Code Changed

Deleted: /ASSET/IMAGES/LARGE/11083-1363-23-1-1-F01.JPEG

- 830–840, doi:10.3189/2012JogI11J118, 2012.
- 1180 Fretwell, P., Pritchard, H. D., Vaughan, D. G., Bamber, J. L., Barrand, N. E., Bell, R., Bianchi, C., Bingham, R. G., Blankenship, D. D., Casassa, G., Catania, G., Callens, D., Conway, H., Cook, A. J., Corr, H. F. J., Damaske, D., Damm, V., Ferraccioli, F., Forsberg, R., Fujita, S., Gim, Y., Gogineni, P., Griggs, J. A., Hindmarsh, R. C. A., Holmlund, P., Holt, J. W., Jacobel, R. W., Jenkins, A., Jokat, W., Jordan, T., King, E. C., Kohler, J., Krabill, W., Riger-Kusk, M., Langley, K. A., Leitchenkov, G., Leuschen, C., Luyendyk, B. P., Matsuoka, K., Mouginot, J., Nitsche, F. O., Nogi, Y., Nost, O. A., Popov, S.
- 1185 V., Rignot, E., Rippin, D. M., Rivera, A., Roberts, J., Ross, N., Siegert, M. J., Smith, A. M., Steinhage, D., Studinger, M., Sun, B., Tinto, B. K., Welch, B. C., Wilson, D., Young, D. A., Xiangbin, C. and Zirizzotti, A.: Bedmap2: Improved ice bed, surface and thickness datasets for Antarctica, *Cryosphere*, 7(1), 375–393, doi:10.5194/tc-7-375-2013, 2013.
- Fürst, J. J., Durand, G., Gillet-Chaulet, F., Merino, N., Tavid, L., Mouginot, J., Gourmelen, N. and Gagliardini, O.: Assimilation of Antarctic velocity observations provides evidence for uncharted pinning points, *Cryosphere*, 9(4), 1427–1443, doi:10.5194/tc-9-1427-2015, 2015.
- 1190 Gardner, A. S., Moholdt, G., Scambos, T., Fahnestock, M., Ligtenberg, S., Van Den Broeke, M. and Nilsson, J.: Increased West Antarctic and unchanged East Antarctic ice discharge over the last 7 years, *Cryosphere*, 12(2), 521–547, doi:10.5194/tc-12-521-2018, 2018.
- Gardner, A. S., Fahnestock, M. A. and Scambos, T. A.: ITS\_LIVE Regional Glacier and Ice Sheet Surface Velocities, Data Arch. Natl. Snow Ice Data Cent., doi:10.5067/6II6VW8LLWJ7, [Accessed 2021](#).
- 1195 Glasser, N. F., Kulesa, B., Luckman, A., Jansen, D., King, E. C., Sammonds, P. R., Scambos, T. A. and Jezek, K. C.: Surface structure and stability of the Larsen C ice shelf, *Antarctic Peninsula, J. Glaciol.*, 55(191), 400–410, doi:10.3189/002214309788816597, 2009.
- Greenbaum, J. S., Blankenship, D. D., Young, D. A., Richter, T. G., Roberts, J. L., Aitken, A. R. A., Legresy, B., Schroeder, D. M., Warner, R. C., van Ommen, T. D. and Siegert, M. J.: Ocean access to a cavity beneath Totten Glacier in East Antarctica, *Nat. Geosci.*, 8(4), 294–298, doi:10.1038/ngeo2388, 2015.
- Grima, C., Greenbaum, J. S., Lopez Garcia, E. J., Soderlund, K. M., Rosales, A., Blankenship, D. D. and Young, D. A.: Radar detection of the brine extent at McMurdo Ice Shelf, Antarctica, and its control by snow accumulation, *Geophys. Res. Lett.*, 43(13), 7011–7018, doi:10.1002/2016GL069524, 2016.
- 1205 Heine, A. J.: Brine in the McMurdo ice shelf, Antarctica, *New Zeal. J. Geol. Geophys.*, 11(4), 829–839, doi:10.1080/00288306.1968.10420755, 1968.
- Inoue, M., Curran, M. A. J., Moy, A. D., Van Ommen, T. D., Fraser, A. D., Phillips, H. E. and Goodwin, I. D.: A glaciochemical study of the 120 m ice core from Mill Island, East Antarctica, *Clim. Past*, 13(5), 437–453, doi:10.5194/cp-13-437-2017, 2017.
- Jenkins, A.: Convection-Driven Melting near the Grounding Lines of Ice Shelves and Tidewater Glaciers, *J. Phys. Oceanogr.*, 41(12), 2279–2294, doi:10.1175/jpo-d-11-03.1, 2011.
- 1210 Kovacs, A., Gow, A. J., Cragin, J. H. and Morey, R. M.: The brine zone in the McMurdo Ice Shelf, Antarctica., *Ann. Glaciol.*, 3, 1–982, doi:10.3189/s0260305500002718, 1982.

Deleted: 19

- Kuipers Munneke, P., Ligtenberg, S. R. M., Van Den Broeke, M. R. and Vaughan, D. G.: Firm air depletion as a precursor of Antarctic ice-shelf collapse, *J. Glaciol.*, 60(220), 205–214, doi:10.3189/2014JoG13J183, 2014.
- 1215 Kuipers Munneke, P., McGrath, D., Medley, B., Luckman, A., Bevan, S., Kulesa, B., Jansen, D., Booth, A., Smeets, P., Hubbard, B., Ashmore, D., Van Den Broeke, M., Sevestre, H., Steffen, K., Shepherd, A. and Gourmelen, N.: Observationally constrained surface mass balance of Larsen C ice shelf, Antarctica, *Cryosphere*, 11(6), 2411–2426, doi:10.5194/tc-11-2411-2017, 2017.
- 1220 Kulesa, B., Jansen, D., Luckman, A. J., King, E. C. and Sammonds, P. R.: Marine ice regulates the future stability of a large Antarctic ice shelf., *Nat. Commun.*, 5, 3707, doi:10.1038/ncomms4707, 2014.
- Kulesa, B., Booth, A. D., O’Leary, M., McGrath, D., King, E. C., Luckman, A. J., Holland, P. R., Jansen, D., Bevan, S. L., Thompson, S. S. and Hubbard, B.: Seawater softening of suture zones inhibits fracture propagation in Antarctic ice shelves, *Nat. Commun.*, 10(1), 1–12, doi:10.1038/s41467-019-13539-x, 2019.
- 1225 Larour, E., Rignot, E., Poinelli, M. and Scheuchl, B.: Physical processes controlling the riftng of Larsen C Ice Shelf, Antarctica, prior to the calving of iceberg A68, *Proc. Natl. Acad. Sci. U. S. A.*, 118(40), doi:10.1073/pnas.2105080118, 2021.
- Liang, Q., Zhou, C. and Zheng, L.: Mapping Basal Melt under the Shackleton Ice Shelf, East Antarctica, from CryoSat-2 Radar Altimetry, *IEEE J. Sel. Top. Appl. Earth Obs. Remote Sens.*, 14, 5091–5099, doi:10.1109/JSTARS.2021.3077359, 2021.
- Luckman, A., Quincey, D. and Bevan, S.: The potential of satellite radar interferometry and feature tracking for monitoring flow rates of Himalayan glaciers, *Remote Sens. Environ.*, 111(2), 172–181, doi:10.1016/j.rse.2007.05.019, 2007.
- 1230 McGrath, D., Steffen, K., Holland, P. R., Scambos, T., Rajaram, H., Abdalati, W., Rignot, E., Steffen, K., McGrath, D., Scambos, T. and Abdalati, W.: The structure and effect of suture zones in the Larsen C Ice Shelf, Antarctica, *J. Geophys. Res. Earth Surf.*, 119(3), 588–602, doi:10.1002/2013jf002935, 2014.
- Miles, B. W. J., Jordan, J. R., Stokes, C. R., Jamieson, S. S. R., Gudmundsson, G. H. and Jenkins, A.: Recent acceleration of Denman Glacier (1972–2017), East Antarctica, driven by grounding line retreat and changes in ice tongue configuration, *Cryosph.*, 15(2), 663–676, doi:10.5194/tc-15-663-2021, 2021.
- 1235 Morlighem, M., Rignot, E., Binder, T., Blankenship, D., Drews, R., Eagles, G., Eisen, O., Ferraccioli, F., Forsberg, R., Fretwell, P., Goel, V., Greenbaum, J. S., Gudmundsson, H., Guo, J., Helm, V., Hofstede, C., Howat, I., Humbert, A., Jokat, W., Karlsson, N. B., Lee, W. S., Matsuoka, K., Millan, R., Mouginot, J., Paden, J., Pattyn, F., Roberts, J., Rosier, S., Ruppel, A., Seroussi, H., Smith, E. C., Steinhage, D., Sun, B., Broeke, M. R. van den, Ommen, T. D. van, Wessem, M. van and Young, D. A.: Deep glacial troughs and stabilizing ridges unveiled beneath the margins of the Antarctic ice sheet, *Nat. Geosci.*, 13(2), 132–137, doi:10.1038/s41561-019-0510-8, 2020.
- Mouginot, J., Scheuch, B. and Rignot, E.: Mapping of Ice Motion in Antarctica Using Synthetic-Aperture Radar Data, *Remote Sens.* 2012, Vol. 4, Pages 2753–2767, 4(9), 2753–2767, doi:10.3390/RS4092753, 2012.
- 1245 Mouginot, J., Rignot, E. and Scheuchl, B.: Continent-Wide, Interferometric SAR Phase, Mapping of Antarctic Ice Velocity, *Geophys. Res. Lett.*, 46(16), 9710–9718, doi:10.1029/2019GL083826, 2019.
- Neal, C. S.: The Dynamics of the Ross Ice Shelf Revealed by Radio Echo-Sounding, *J. Glaciol.*, 24(90), 295–307,

- doi:10.3189/s0022143000014817, 1979.
- 1250 Peters, M. E., Blankenship, D. D., Carter, S. P., Kempf, S. D., Young, D. A. and Holt, J. W.: Along-track focusing of airborne radar sounding data from west antarctica for improving basal reflection analysis and layer detection, *IEEE Trans. Geosci. Remote Sens.*, 45(9), 2725–2736, doi:10.1109/TGRS.2007.897416, 2007.
- Rignot, E., Mouginot, J. and Scheuchl, B.: Ice Flow of the Antarctic Ice Sheet, *Science* (80-. ), 333(6048), 1427–1430, doi:10.1126/science.1208336, 2011.
- 1255 Rignot, E., Jacobs, S., Mouginot, J., Scheuchl, B., Fretwell, P., Pritchard, H. D., Vaughan, D. G., Bamber, J. L., Barrand, N. E., Bell, R., Bianchi, C., Bingham, R. G., Blankenship, D. D., Casassa, G., Catania, G., Callens, D., Conway, H., Cook, A. J., Corr, H. F. J., Damaske, D., Damm, V., Ferraccioli, F., Forsberg, R., Fujita, S., Gim, Y., Gogineni, P., Griggs, J. A., Hindmarsh, R. C. A., Holmlund, P., Holt, J. W., Jacobel, R. W., Jenkins, A., Jokat, W., Jordan, T., King, E. C., Kohler, J., Krabill, W., Riger-Kusk, M., Langley, K. A., Leitchenkov, G., Leuschen, C., Luyendyk, B. P., Matsuoka, K., Mouginot, J., Nitsche, F. O., Nogi, Y., Nost, O. A. and Popov, S. V.: Ice-shelf melting around Antarctica., *Science*, 341(6143), 266–70, doi:10.1126/science.1235798, 2013.
- 1260 Rignot, E., Mouginot J. and Scheuchl., B.: MEASURES InSAR-Based Antarctica Ice Velocity Map, Version 2., NASA Natl. Snow Ice Data Cent. Distrib. Act. Arch. Cent., doi:https://doi.org/10.5067/D7GK8F5J8M8R, 2017.
- Rignot, E., Mouginot, J., Scheuchl, B., van den Broeke, M., van Wessem, M. J. and Morlighem, M.: Four decades of Antarctic Ice Sheet mass balance from 1979–2017, *Proc. Natl. Acad. Sci.*, 116(4), 1095–1103, doi:10.1073/pnas.1812883116, 2019.
- 1265 Risk, G. F. and Hochstein, M. P.: Subsurface Measurements on the Memurdo Ice Shelf, Antarctica, *New Zeal. J. Geol. Geophys.*, 10(2), 484–497, doi:10.1080/00288306.1967.10426753, 1967.
- Scambos, T. A., Haran, T. M., Fahnestock, M. A., Painter, T. H. and Bohlander, J.: MODIS-based Mosaic of Antarctica (MOA) data sets: Continent-wide surface morphology and snow grain size, *Remote Sens. Environ.*, 111(2–3), 242–257, doi:10.1016/J.RSE.2006.12.020, 2007.
- 1270 Silvano, A., Rintoul, S. and Herraiz-Borreguero, L.: Ocean-Ice Shelf Interaction in East Antarctica, *Oceanography*, 29(4), 130–143, doi:10.5670/oceanog.2016.105, 2016.
- Smith, B. M. E. and Evans, S.: Radio Echo Sounding: Absorption and Scattering by Water Inclusion and Ice Lenses, *J. Glaciol.*, 11(61), 133–146, doi:10.3189/s0022143000022541, 1972.
- Stephenson, S. N., Boulevard, F. and Zwally, H. J.: Ice-shelf topography and structure determined using satellite-radar altimetry and landsat imagery, *Ann. Glaciol.*, 12, 162–169, 1989.
- 1275 Stokes, C. R., Sanderson, J. E., Miles, B. W. J., Jamieson, S. S. R. and Leeson, A. A.: Widespread distribution of supraglacial lakes around the margin of the East Antarctic Ice Sheet, *Sci. Rep.*, 9(1), 1–14, doi:10.1038/s41598-019-50343-5, 2019.
- Thomas, R. H.: Liquid Brine in Ice Shelves, *J. Glaciol.*, 14(70), 125–136, doi:10.3189/s0022143000013459, 1975.
- Vaughan, D. G., Mantripp, D. R., Sievers, J. and Doake, C. S. M.: A synthesis of remote sensing data on Wilkins Ice Shelf, Antarctica, *Ann. Glaciol.*, 17, 211–218, doi:10.3189/s0260305500012866, 1993.
- 1280 Walford, M. E. R.: Radio echo sounding through an ice shelf, *Nature*, 204(4956), 317–319, doi:10.1038/204317a0, 1964.

Wei, W., Blankenship, D. D., Greenbaum, J. S., Gourmelen, N., Dow, C. F., Richter, T. G., Greene, C. A., Young, D. A., Lee, S. H., Kim, T. W., Lee, W. S. and Assmann, K. M.: Getz Ice Shelf melt enhanced by freshwater discharge from beneath the West Antarctic Ice Sheet, *Cryosphere*, 14(4), 1399–1408, doi:10.5194/tc-14-1399-2020, 2020.

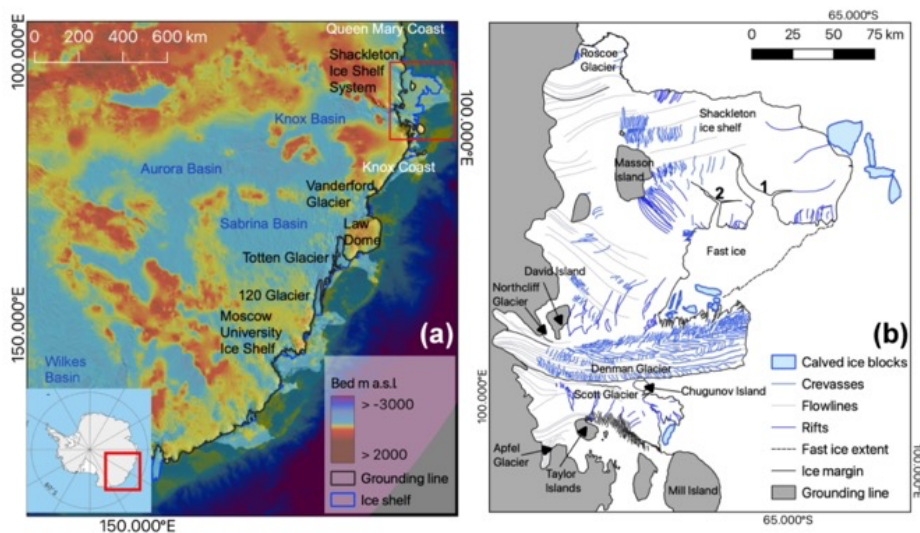
1285 Williams, G. D., Meijers, A. J. S., Poole, A., Mathiot, P., Tamura, T. and Klocker, A.: Late winter oceanography off the Sabrina and BANZARE coast (117-128°E), East Antarctica, *Deep. Res. Part II Top. Stud. Oceanogr.*, 58(9–10), 1194–1210, doi:10.1016/j.dsr2.2010.10.035, 2011.

Young, D. A., Wright, A. P., Roberts, J. L., Warner, R. C., Young, N. W., Greenbaum, J. S., Schroeder, D. M., Holt, J. W., Sugden, D. E., Blankenship, D. D., van Ommen, T. D. and Siegert, M. J.: A dynamic early East Antarctic Ice Sheet suggested by ice-covered fjord landscapes, *Nature*, 474, 72 [online] Available from: <https://doi.org/10.1038/nature10114>, 2011.

1290 Young, N.: Surface velocities of Denman Glacier, Antarctica, derived from Landsat imagery, *Ann. Glaciol.*, 12, 218, 1989.

## Figures

Formatted: Font: Bold



1295 **Figure 1:** (a) Area of focus in the regional context of the Aurora and Wilkes subglacial basins, location shown in inset (Background: BedMachine V2 (Morlighem et al., 2020)). (b) The Shackleton system overview in February 2021. All features mapped from Sentinel 2A and 2B imagery acquired 05<sup>th</sup> – 27<sup>th</sup> February 2021.

Deleted: 2021

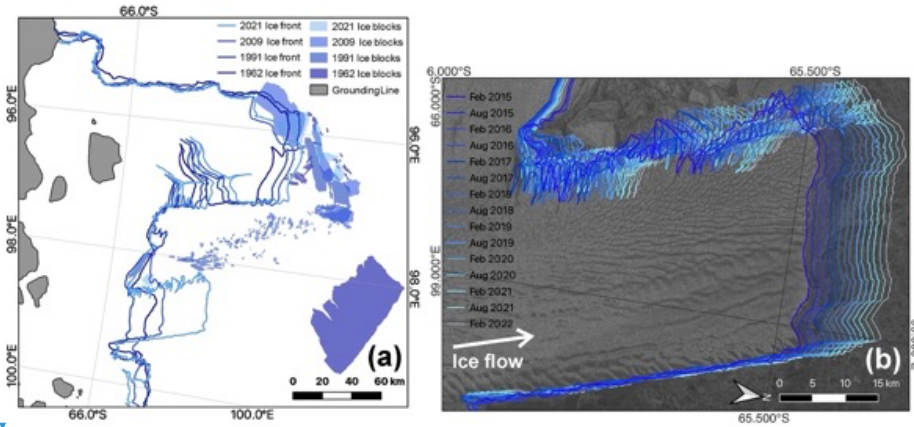
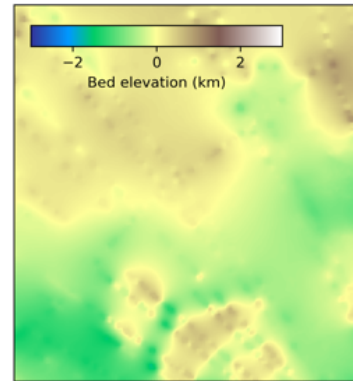
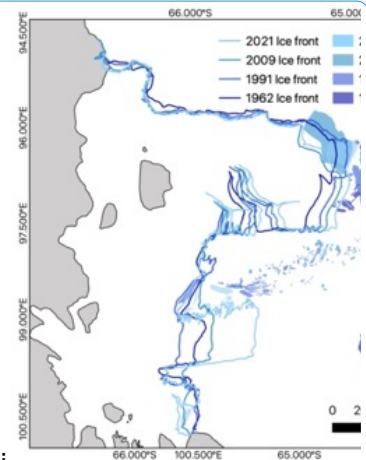


Figure 2; (a) Ice front positions of the Queen Mary and Knox coasts since 1962, including the large iceberg hypothesised to have calved from the Denman tongue in the 1940s. Position and blocks mapped from 16<sup>th</sup> May 1962 – ARGON KH5, 10<sup>th</sup> -12th February 1991 – Landsat 5 TM, 1<sup>st</sup> November – 28<sup>th</sup> February 2009 – Modis MOA (Scambos et al., 2007) and 5<sup>th</sup> – 27<sup>th</sup> February 2021 – Sentinel 2A and 2B. (b) Denman Glacier biannual ice front position mapped in February and August from 2015 through 2022 (Background: Sentinel 1a acquired 27<sup>th</sup> February 2015).



Deleted:  
Figure 2: BISCLES model domain and bedrock elevation (Morlighem et al., 2020).



Deleted:

Deleted: 3

Deleted: 2021

Deleted: 14

Deleted: 21



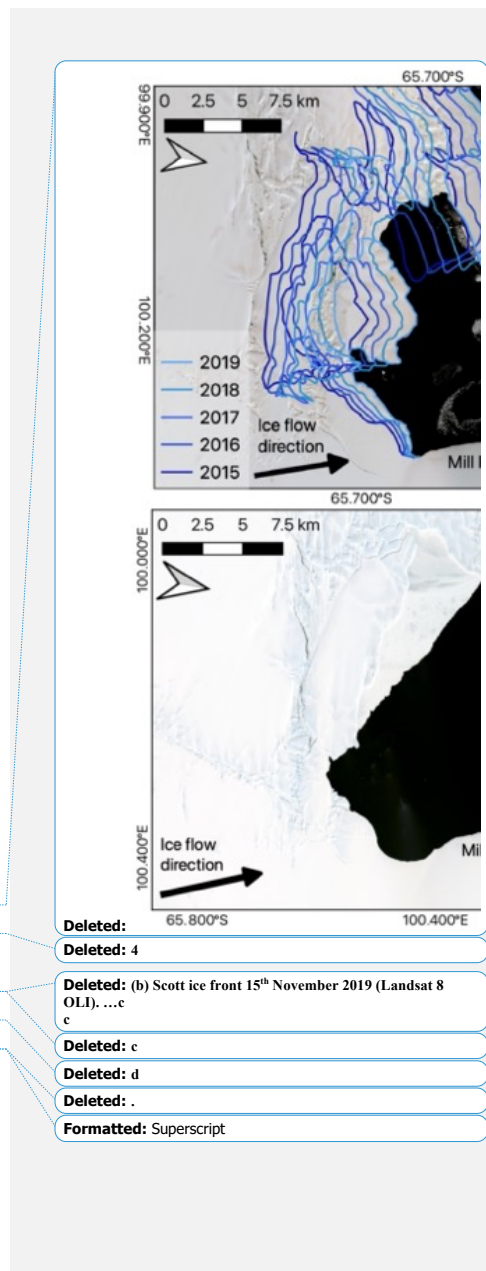
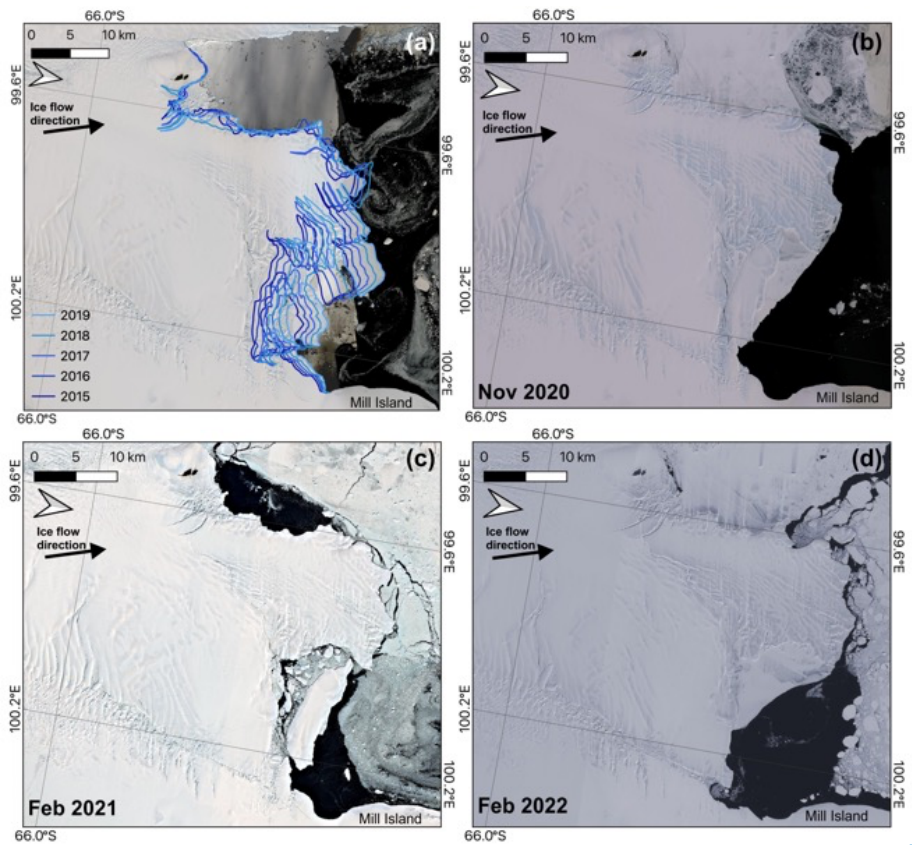


Figure 3: (a) Scott ice front position between 2015 and 2019 mapped from Landsat 8 OLI acquired on 16<sup>th</sup> February 2019, 1<sup>st</sup> February 2018, 24<sup>th</sup> February 2016 and 7<sup>th</sup> February 2015 and from Sentinel 2A acquired on 23<sup>rd</sup> February 2017 (Background: Landsat 8 OLI – 16<sup>th</sup> February 2019). (b) Scott ice front 26<sup>th</sup> November 2020, the central portion of the front has lost some of the blocks held in place by fast ice and an area immediately to the south of Mill Island (Landsat 8 OLI), (c) Scott ice front 27<sup>th</sup> February 2021, the fast ice has broken up and a larger block is separated (Sentinel 2B), (d) Scott ice front 21<sup>st</sup> February 2022, (Sentinel 2B).

- Deleted:
- Deleted: 4
- Deleted: (b) Scott ice front 15<sup>th</sup> November 2019 (Landsat 8 OLI). ...c
- Deleted: c
- Deleted: d
- Deleted: .
- Formatted: Superscript

315

320

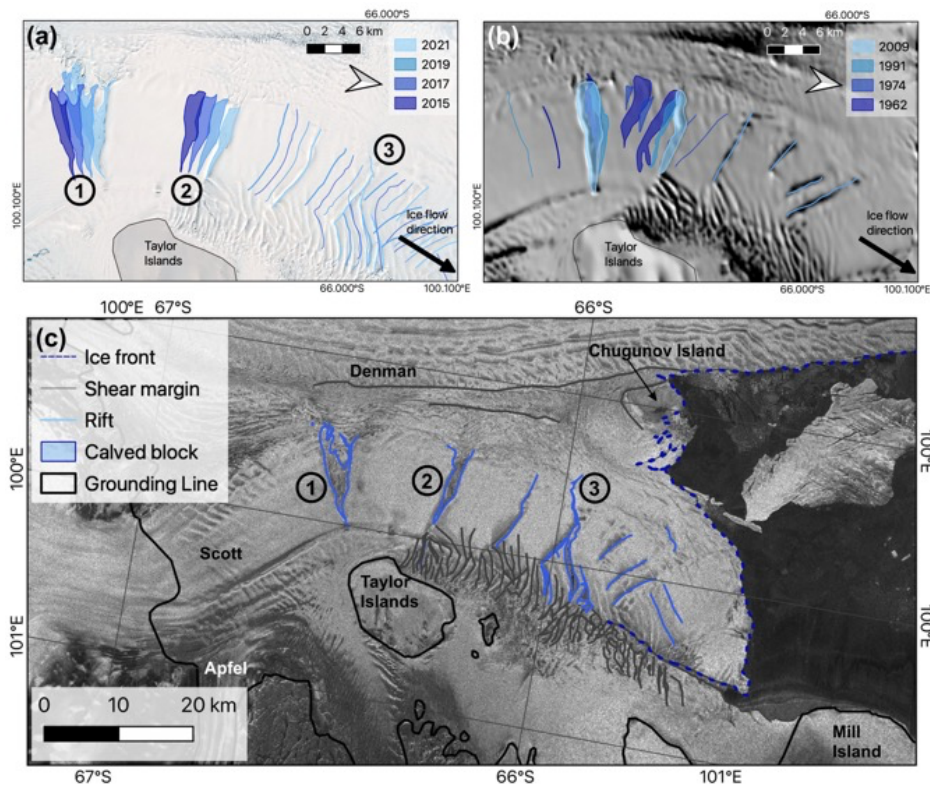
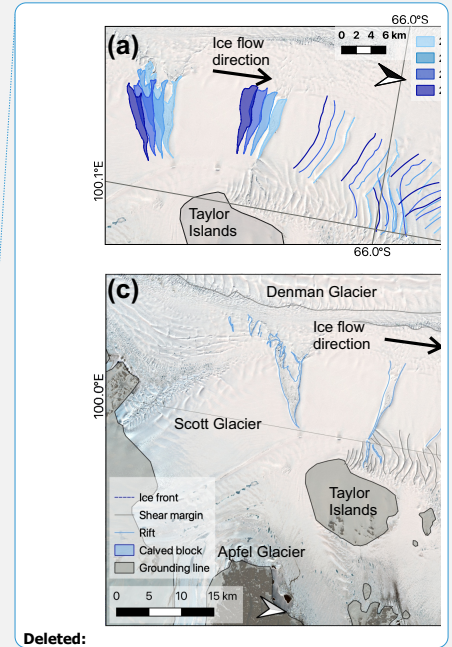


Figure 4: Evolution of the rifts on Scott Glaciers from (a) 2015-2021 mapped from Sentinel 2B acquired 27th February 2021, Landsat 8 OLI acquired 16<sup>th</sup> February 2019 and 25<sup>th</sup> March 2015 and from Sentinel 2A acquired 23<sup>rd</sup> February 2017 (Background: Sentinel 2B acquired 27th February 2021) and (b) 1962-2009 mapped from ARGON KH5 acquired 16<sup>th</sup> May 1962, Landsat 1 MMS acquired 27<sup>th</sup> February 1974 and Landsat 5 TM acquired 10<sup>th</sup> -12<sup>th</sup> February 1991 and from MODIS MOA acquired 1<sup>st</sup> November – 28<sup>th</sup> February 2009 – Modis MOA (Scambos et al., 2007) (Background: MODIS MOA). (c) The floating portion of Scott Glacier in June 2022, highlighting the iceberg that calved from the western front in April 2022 and the rifting across the eastern portion of the front towards Chugunov Island (Background: Sentinel 1A acquired 6th June 2022).



Deleted:

Deleted: 5

Deleted: February

Deleted: 1

Deleted: eastern

Deleted: 0

Deleted: s

Deleted: joining together

Deleted: 2B

Deleted: 27

Deleted: February

Deleted: 1

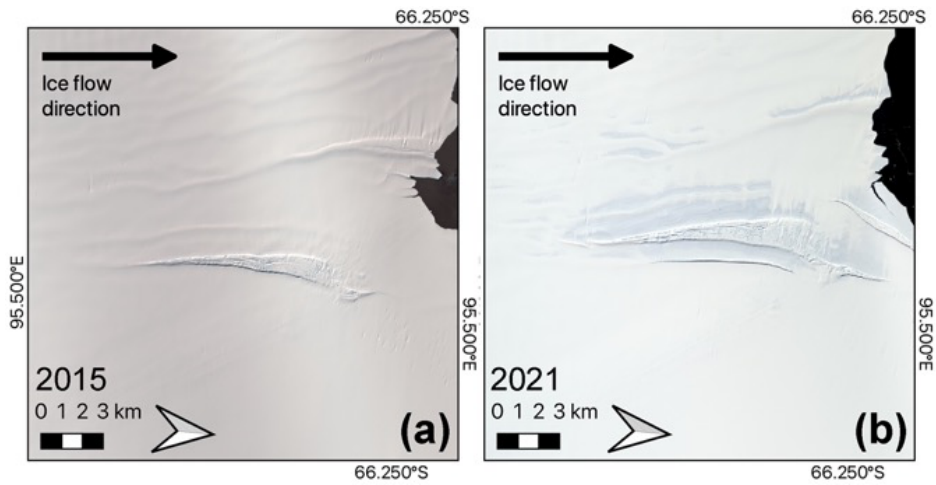
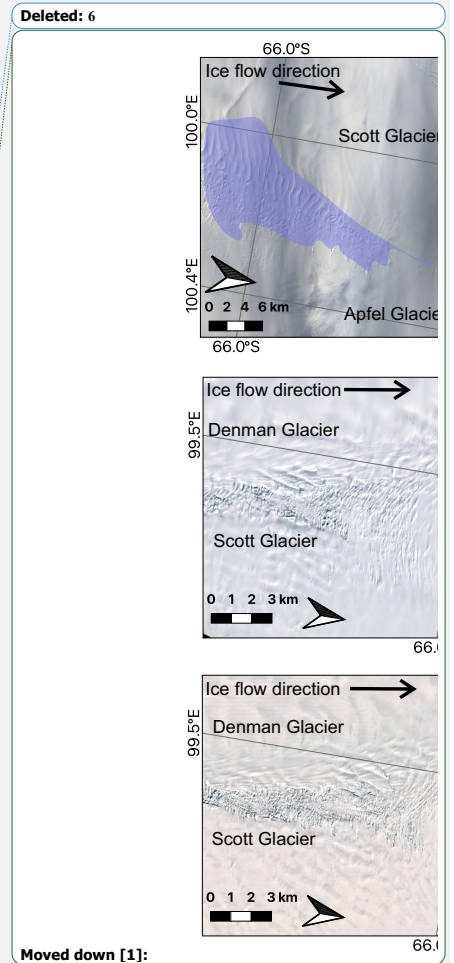
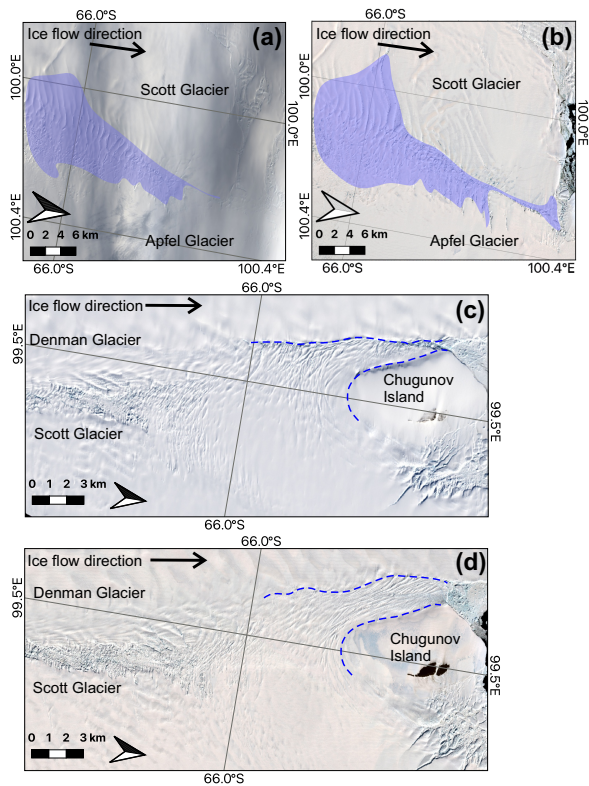


Figure 5: Rift opening in the vicinity of the Shackleton Roscoe Glacier shear margin between (a) 2015 (Background: Landsat 8 OLI acquired 14th March 2015) and (b) 2021 (Sentinel 2B acquired 13<sup>th</sup> February 2021).

355





**Figure 6:** (a) The 2015 extent of the Scott-Apfel Glacier shear margin highlighted in blue (Background Landsat 8 OLI acquired 25<sup>th</sup> March). (b) The 2021 extent of the Scott-Apfel Glacier shear margin highlighted in blue (Background: Sentinel 2B 13<sup>th</sup> February 2021). (c) Scott-Denman Glacier shear margin in 2015, the dashed blue line highlights the position and shape of the margin. (Background: Landsat 8 OLI acquired February 2015). (d) The Scott-Denman Glacier shear margin in 2021, the dashed blue line highlights the widening of the shear margin into the Denman Glacier (Background: Sentinel 2B acquired 27<sup>th</sup> February 2021).

**Moved (insertion) [1]**

**Formatted: Centred**

**Formatted Table**

**Deleted:** Figure 7: (a) The 2015 extent of the Scott-Apfel Glacier shear margin highlighted in blue (Background Landsat 8 OLI acquired 25<sup>th</sup> March). (b) The 2021 extent of the Scott-Apfel Glacier shear margin highlighted in blue (Background: Sentinel 2B 13<sup>th</sup> February 2021). (c) Scott-Denman Glacier shear margin in 2015, the dashed blue line highlights the position and shape of the margin. (Background: Landsat 8 OLI acquired February 2015). (d) The Scott-Denman Glacier shear margin in 2021, the dashed blue line highlights the widening of the shear margin into the Denman Glacier (Background: Sentinel 2B acquired 27<sup>th</sup> February 2021). ...

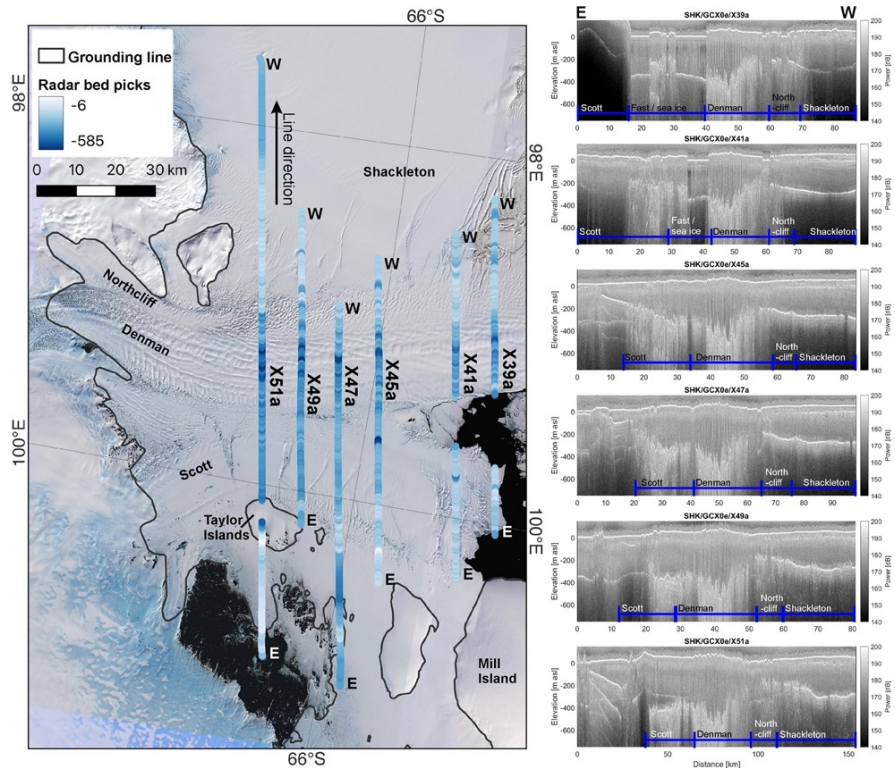


Figure 7: (a) The location and ice base below sea level of 6 ICECAP radar lines acquired in December 2016 (Background Sentinel 2A acquired 23<sup>rd</sup> February and 1<sup>st</sup> March 2017). (b) Annotated ICECAP radar lines (position and east-west line direction shown in a).

Formatted Table

Formatted: Superscript

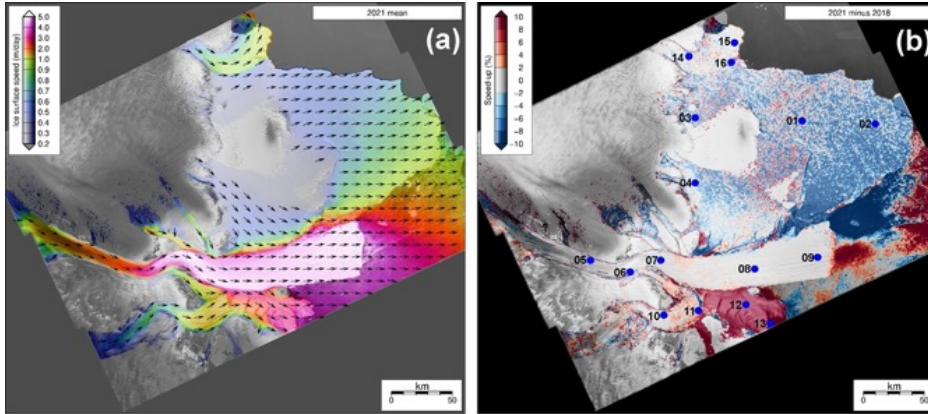
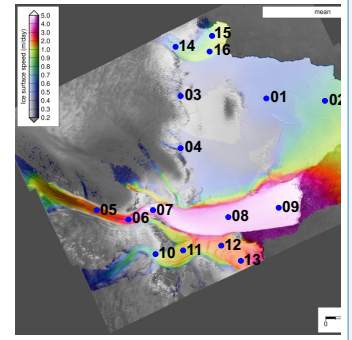


Figure 8: (a) Mean speed for 2022 with velocity arrows and (b) percentage difference in mean speed between 2021 and 2018, scaled between +/- 10%, with point locations illustrating the ice speed timeseries in Figure 10.

375

Formatted: Centred



Deleted:

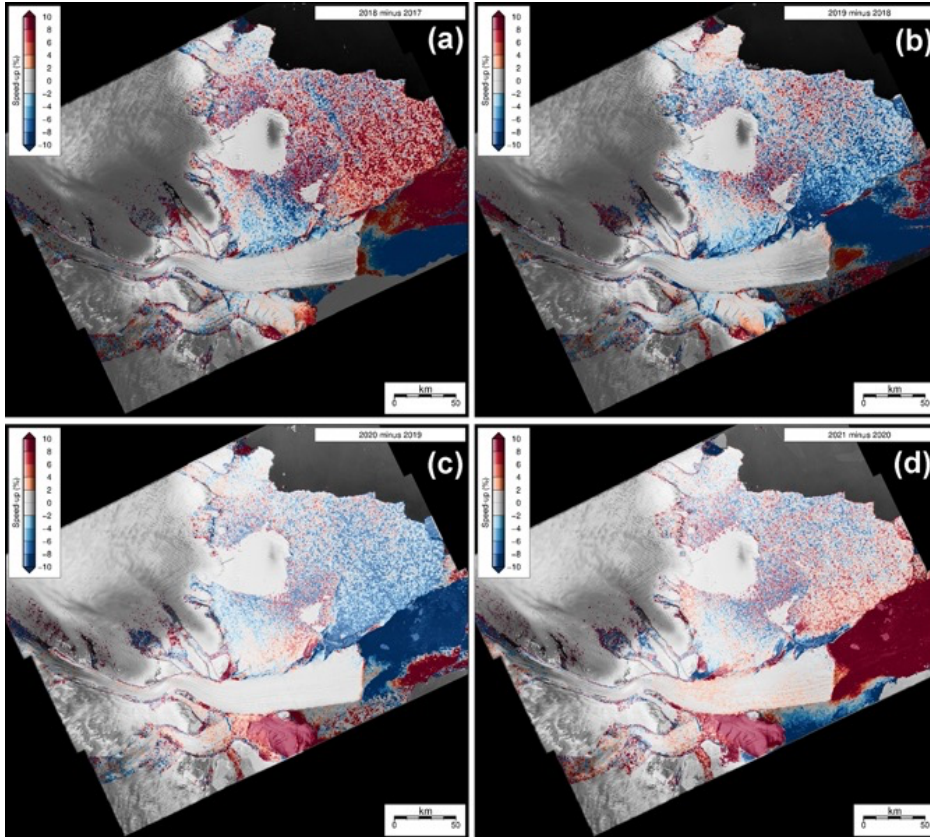
Formatted: Font: 9 pt

Formatted: Font: 9 pt

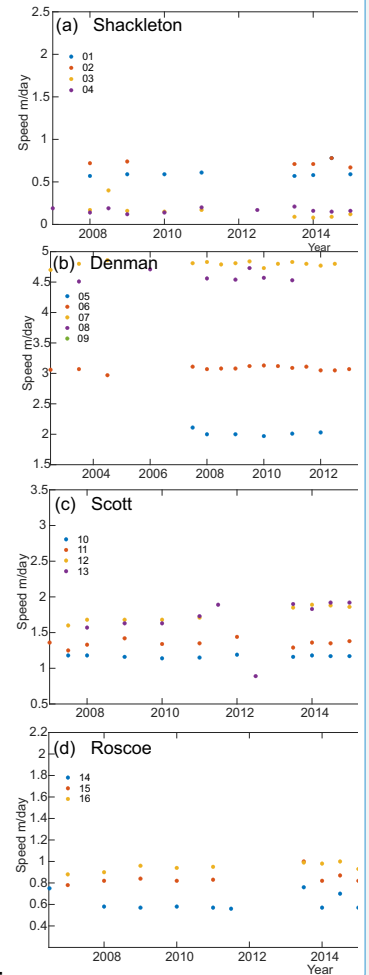
Formatted: Font: 9 pt, Bold

Deleted: Figure 8: (a) Mean speed, with point locations for Fig. 9, and (b) difference in mean speed between 2020 and 2019.

Formatted: Font: 9 pt, Bold



380 **Figure 3:** Percentage difference in mean speed between (a) 2018-17, (b) 2019-18, (c) 2020-19 and (d) 2021-20 scaled between +/- 10%.



**Deleted:**

**Formatted:** Centred

**Deleted:** 9

**Deleted:** Time series of speed at point locations (shown in Figure 10a) across the Denman-Scott-Shackleton system derived from Sentinel 1 between 2017 and 2021 (uncertainties in velocity magnitude are around 0.2 m/day following (Benn et al., 2019)) and extended back to 2002 using Measures and ITS\_LIVE where available (Rignot et al., 2017).

**Formatted:** Font: 9 pt, Bold

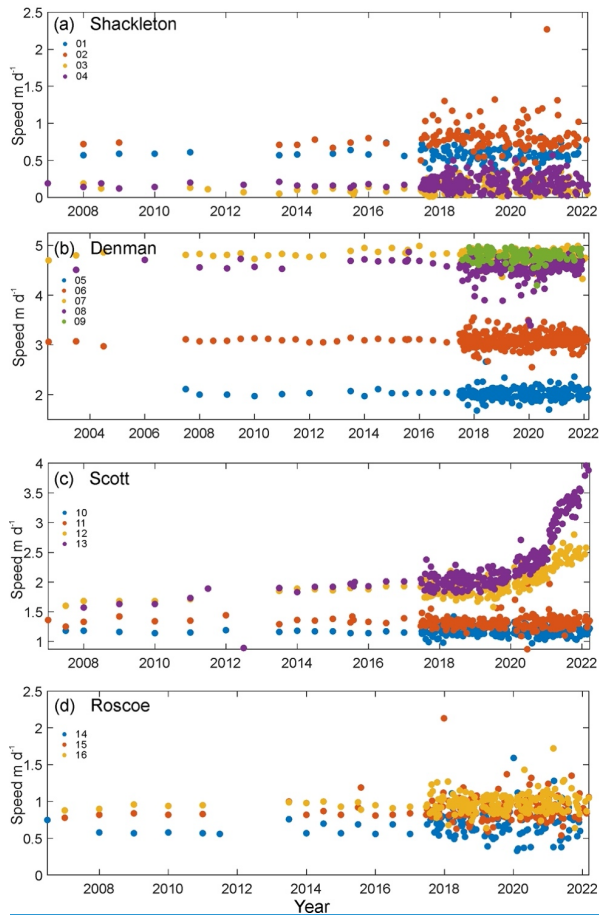


**Figure 10:** Time series of speed at point locations (shown in Figure 8a) across the Denman-Scott-Shackleton system derived from Sentinel 1 between 2017 and 2021 (uncertainties in velocity magnitude are around  $0.2 \text{ m day}^{-1}$  following (Benn et al., 2019)) and extended back to 2002 using Measures and ITS LIVE where available (Rignot et al., 2017).

Formatted: Centred

Formatted Table

Formatted: Font: 9 pt

Formatted: Font: (Default) Times New Roman



400

Figure 10: Time series of speed at point locations (shown in Figure 10a) across the Denman-Scott-Shackleton system derived from Sentinel 1 between 2017 and 2021 (uncertainties in velocity magnitude are around  $0.2 \text{ m day}^{-1}$  following (Benn et al., 2019)) and extended back to 2002 using Measures and ITS LIVE where available (Rignot et al., 2017).

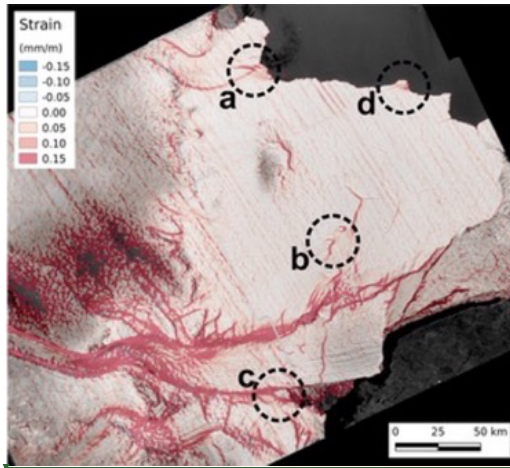


Figure 11: Magnitude of the principal strain rate of the Denman-Scott-Shackleton system derived from Sentinel-1 data. N.B. The feature down flow of pinning point c on the Denman Tongue is an artefact, we see no evidence of rifting in the remote sensing data in this region (e.g., Fig. 2b, 7a).

405

Formatted: Font: 9 pt, Bold

Formatted: Font: 9 pt, Bold

Formatted: Font: 9 pt, Bold

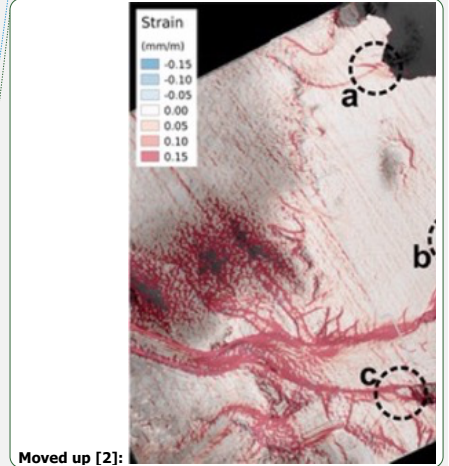
Formatted: Font: 9 pt, Bold

Formatted: Font: 9 pt, Bold

Moved (insertion) [2]

Formatted Table

Formatted: Font colour: Black, Pattern: Clear (White)



Moved up [2]:

Formatted: Centred

Deleted: Figure 10: Magnitude of the principal strain rate of the Denman-Scott-Shackleton system derived from Sentinel-1 data.

Deleted:

¶

¶

[34]

Deleted: Figure 11: The results of the model calibration over subset of the domain (a) modelled speed, (b) difference between modelled speed and observed speed, (c) basal friction and (d) the stiffness factor.

[35]

Page 1: [1] Deleted Sarah Thompson 22/04/2022 15:04:00

Page 1: [1] Deleted Sarah Thompson 22/04/2022 15:04:00

Page 1: [1] Deleted Sarah Thompson 22/04/2022 15:04:00

Page 1: [2] Formatted Sarah Thompson 15/06/2022 10:28:00

Superscript

Page 1: [2] Formatted Sarah Thompson 15/06/2022 10:28:00

Superscript

Page 1: [3] Formatted Sarah Thompson 15/06/2022 10:28:00

Superscript

Page 1: [3] Formatted Sarah Thompson 15/06/2022 10:28:00

Superscript

Page 1: [3] Formatted Sarah Thompson 15/06/2022 10:28:00

Superscript

Page 1: [3] Formatted Sarah Thompson 15/06/2022 10:28:00

Superscript

Page 1: [4] Deleted Sarah Thompson 20/06/2022 10:31:00

Page 1: [4] Deleted Sarah Thompson 20/06/2022 10:31:00

Page 1: [4] Deleted Sarah Thompson 20/06/2022 10:31:00

Page 1: [4] Deleted Sarah Thompson 20/06/2022 10:31:00

Page 1: [5] Deleted Sarah Thompson 16/05/2022 12:26:00

Page 1: [5] Deleted Sarah Thompson 16/05/2022 12:26:00

Page 1: [5] Deleted Sarah Thompson 16/05/2022 12:26:00

Page 1: [5] Deleted Sarah Thompson 16/05/2022 12:26:00

Page 1: [6] Deleted Sarah Thompson 09/02/2022 14:20:00

Page 1: [6] Deleted Sarah Thompson 09/02/2022 14:20:00

Page 1: [6] Deleted Sarah Thompson 09/02/2022 14:20:00

Page 1: [6] Deleted Sarah Thompson 09/02/2022 14:20:00

Page 1: [6] Deleted Sarah Thompson 09/02/2022 14:20:00

Page 1: [6] Deleted Sarah Thompson 09/02/2022 14:20:00

Page 1: [6] Deleted Sarah Thompson 09/02/2022 14:20:00

Page 1: [6] Deleted Sarah Thompson 09/02/2022 14:20:00

Page 1: [6] Deleted Sarah Thompson 09/02/2022 14:20:00

Page 1: [6] Deleted Sarah Thompson 09/02/2022 14:20:00

Page 1: [6] Deleted Sarah Thompson 09/02/2022 14:20:00

Page 1: [6] Deleted Sarah Thompson 09/02/2022 14:20:00

▼  
▲  
**Page 1: [6] Deleted Sarah Thompson 09/02/2022 14:20:00**

▼  
▲  
**Page 5: [7] Deleted Sarah Thompson 09/02/2022 14:22:00**

▼  
▲  
**Page 5: [8] Deleted Sarah Thompson 16/05/2022 12:49:00**

▼  
▲  
**Page 5: [9] Deleted Sarah Thompson 16/05/2022 12:50:00**

▼  
▲  
**Page 7: [10] Formatted Sarah Thompson 13/06/2022 14:34:00**

Font: 10 pt

▼  
▲  
**Page 7: [10] Formatted Sarah Thompson 13/06/2022 14:34:00**

Font: 10 pt

▼  
▲  
**Page 7: [11] Formatted Sarah Thompson 13/06/2022 14:34:00**

Font: 10 pt

▼  
▲  
**Page 7: [11] Formatted Sarah Thompson 13/06/2022 14:34:00**

Font: 10 pt

▼  
▲  
**Page 7: [11] Formatted Sarah Thompson 13/06/2022 14:34:00**

Font: 10 pt

▼  
▲  
**Page 7: [12] Deleted Sarah Thompson 22/04/2022 12:28:00**

▼  
▲  
**Page 7: [12] Deleted Sarah Thompson 22/04/2022 12:28:00**

▼  
▲  
**Page 7: [12] Deleted Sarah Thompson 22/04/2022 12:28:00**

▼  
▲  
**Page 7: [12] Deleted Sarah Thompson 22/04/2022 12:28:00**

▼  
▲  
**Page 7: [12] Deleted Sarah Thompson 22/04/2022 12:28:00**

▼  
▲  
**Page 7: [13] Deleted Sarah Thompson 22/04/2022 13:08:00**

▼  
▲  
**Page 7: [13] Deleted Sarah Thompson 22/04/2022 13:08:00**

▼  
▲  
**Page 7: [14] Deleted Tvler Pelle 14/06/2022 10:53:00**

▼  
▲  
**Page 7: [15] Deleted Sarah Thompson 22/04/2022 13:10:00**

▼  
▲  
**Page 7: [15] Deleted Sarah Thompson 22/04/2022 13:10:00**

▼  
▲  
**Page 7: [15] Deleted Sarah Thompson 22/04/2022 13:10:00**

▼  
▲  
**Page 7: [15] Deleted Sarah Thompson 22/04/2022 13:10:00**

▼  
▲  
**Page 7: [15] Deleted Sarah Thompson 22/04/2022 13:10:00**

▼  
▲  
**Page 7: [15] Deleted Sarah Thompson 22/04/2022 13:10:00**

▼  
▲  
**Page 7: [16] Deleted Tyler Pelle 14/06/2022 10:55:00**

▼  
▲  
**Page 7: [16] Deleted Tyler Pelle 14/06/2022 10:55:00**

▼  
▲  
**Page 7: [16] Deleted Tyler Pelle 14/06/2022 10:55:00**

▼  
▲  
**Page 7: [16] Deleted Tyler Pelle 14/06/2022 10:55:00**

▼  
▲  
**Page 7: [16] Deleted Tyler Pelle 14/06/2022 10:55:00**

▼  
▲  
**Page 7: [17] Deleted Tyler Pelle 14/06/2022 10:59:00**

▼  
▲  
**Page 7: [17] Deleted Tyler Pelle 14/06/2022 10:59:00**

▼  
▲  
**Page 7: [18] Deleted Sarah Thompson 20/06/2022 11:47:00**

▼  
▲  
**Page 7: [18] Deleted Sarah Thompson 20/06/2022 11:47:00**

▼  
▲  
**Page 7: [20] Deleted Sarah Thompson 09/02/2022 15:53:00**

▼  
▲  
**Page 7: [20] Deleted Sarah Thompson 09/02/2022 15:53:00**

▼  
▲  
**Page 7: [20] Deleted Sarah Thompson 09/02/2022 15:53:00**

▼  
▲  
**Page 7: [20] Deleted Sarah Thompson 09/02/2022 15:53:00**

▼  
▲  
**Page 7: [21] Deleted Sarah Thompson 18/03/2022 13:54:00**

▼  
▲  
**Page 7: [21] Deleted Sarah Thompson 18/03/2022 13:54:00**

▼  
▲  
**Page 7: [21] Deleted Sarah Thompson 18/03/2022 13:54:00**

▼  
▲  
**Page 7: [22] Deleted Tyler Pelle 14/06/2022 11:01:00**

▼  
▲  
**Page 7: [22] Deleted Tyler Pelle 14/06/2022 11:01:00**

▼  
▲  
**Page 8: [23] Deleted Sarah Thompson 09/02/2022 15:50:00**

▼  
▲  
**Page 8: [23] Deleted Sarah Thompson 09/02/2022 15:50:00**

▼  
▲  
**Page 8: [24] Deleted Sarah Thompson 18/03/2022 13:47:00**

▼  
▲  
**Page 8: [24] Deleted Sarah Thompson 18/03/2022 13:47:00**

▼  
▲  
**Page 8: [25] Deleted Sarah Thompson 18/03/2022 13:48:00**

▼  
▲  
**Page 8: [25] Deleted Sarah Thompson 18/03/2022 13:48:00**

▼  
▲  
**Page 8: [25] Deleted Sarah Thompson 18/03/2022 13:48:00**

▼  
▲  
**Page 8: [26] Deleted Sarah Thompson 09/02/2022 16:07:00**

▼  
▲  
**Page 8: [26] Deleted Sarah Thompson 09/02/2022 16:07:00**

▼  
▲  
**Page 8: [26] Deleted Sarah Thompson 09/02/2022 16:07:00**

▼  
▲  
**Page 8: [26] Deleted Sarah Thompson 09/02/2022 16:07:00**

▼  
▲  
**Page 8: [26] Deleted Sarah Thompson 09/02/2022 16:07:00**

▼  
▲  
**Page 8: [26] Deleted Sarah Thompson 09/02/2022 16:07:00**

▼  
▲  
**Page 8: [27] Deleted Sarah Thompson 09/02/2022 14:23:00**

▼  
▲  
**Page 8: [28] Deleted Sarah Thompson 18/03/2022 08:42:00**

▼  
▲  
**Page 8: [28] Deleted Sarah Thompson 18/03/2022 08:42:00**

▼  
▲  
**Page 8: [28] Deleted Sarah Thompson 18/03/2022 08:42:00**

▼  
▲  
**Page 8: [28] Deleted Sarah Thompson 18/03/2022 08:42:00**

▼  
▲  
**Page 8: [28] Deleted Sarah Thompson 18/03/2022 08:42:00**

▼  
▲  
**Page 8: [28] Deleted Sarah Thompson 18/03/2022 08:42:00**

▼  
▲  
**Page 8: [28] Deleted Sarah Thompson 18/03/2022 08:42:00**

▼  
▲  
**Page 8: [28] Deleted Sarah Thompson 18/03/2022 08:42:00**

▲  
**Page 8: [29] Formatted Sarah Thompson 17/06/2022 12:20:00**

Font: Not Italic

▲  
**Page 8: [29] Formatted Sarah Thompson 17/06/2022 12:20:00**

Font: Not Italic

▲  
**Page 8: [29] Formatted Sarah Thompson 17/06/2022 12:20:00**

Font: Not Italic

▲  
**Page 8: [29] Formatted Sarah Thompson 17/06/2022 12:20:00**

Font: Not Italic

▲  
**Page 8: [29] Formatted Sarah Thompson 17/06/2022 12:20:00**

Font: Not Italic

▲  
**Page 8: [29] Formatted Sarah Thompson 17/06/2022 12:20:00**

Font: Not Italic

▲  
**Page 8: [29] Formatted Sarah Thompson 17/06/2022 12:20:00**

Font: Not Italic

▲  
**Page 8: [29] Formatted Sarah Thompson 17/06/2022 12:20:00**

Font: Not Italic

▲  
**Page 8: [29] Formatted Sarah Thompson 17/06/2022 12:20:00**

Font: Not Italic

▲  
**Page 8: [29] Formatted Sarah Thompson 17/06/2022 12:20:00**

Font: Not Italic

▲  
**Page 8: [29] Formatted Sarah Thompson 17/06/2022 12:20:00**

Font: Not Italic

▲  
**Page 8: [29] Formatted Sarah Thompson 17/06/2022 12:20:00**

Font: Not Italic

▲  
**Page 8: [29] Formatted Sarah Thompson 17/06/2022 12:20:00**

Font: Not Italic

▲  
**Page 8: [29] Formatted Sarah Thompson 17/06/2022 12:20:00**

Font: Not Italic

▲  
**Page 8: [29] Formatted Sarah Thompson 17/06/2022 12:20:00**

Font: Not Italic

▲  
**Page 8: [30] Deleted Sarah Thompson 16/06/2022 11:58:00**



▲ Page 10: [31] Deleted Sarah Thompson 17/06/2022 12:33:00

▼ Page 10: [32] Deleted Tyler Pelle 14/06/2022 11:29:00

▲ Page 10: [33] Deleted Tyler Pelle 14/06/2022 11:30:00

▼ Page 25: [34] Deleted Sarah Thompson 20/06/2022 10:45:00

▲ Page 25: [35] Deleted Sarah Thompson 18/03/2022 13:40:00